# Raman Spectroscopy, Microscopy and Imaging

Q&A

thermo scientific

Raman spectroscopy is now well established as one of the most powerful and versatile techniques for a diverse range of applications in both research and analytical laboratories. Integrating the Raman spectrometer with a light microscope offers a unique ability to noninvasively characterize chemically complex and spatially inhomogeneous samples with a sub-micron spatial resolution. Modern confocal Raman microscopy and imaging, which allows one to obtain two- and three-dimensional spectrochemical images of samples in various states and forms, has become an indispensable research method for scientific communities, from physicists to chemists, to criminalists, to geologists, to biologists, to medics, etc.

The Q&A for Raman Spectroscopy, Microscopy and Imaging aims to familiarize a wide circle of experimenters with the fundamentals of modern Raman spectroscopy and microscopy, in particular. The Q&A consists of four sections: 1) Introduction to Raman Spectroscopy, 2) Basic Theory and Terminology, 3) Raman Spectrometer and Instrumentation, 4) Raman Microscopy and Instrumentation.

The first section outlines the physics of the interaction of light and molecules and the experimental discovery of the Raman effect.

The second section introduces the basics of Raman scattering and Raman spectroscopy. It considers the relationship between the properties of molecules and their Raman activity, points out the complementary nature of Raman and FTIR spectroscopies, and summarizes the major benefits of Raman spectroscopy. Special attention is drawn to the phenomenon of fluorescence and how it interferes with Raman spectra.

In the third section, the key components of a Raman spectrometer are specified, the basic principles of their operations are described, and their main parameters are characterized. The importance of choosing the most optimal excitation (laser) wavelength and finely controlling its power is emphasized in order to obtain the most informative Raman spectral data for a specific application.

The final fourth section introduces the fundamentals and practical aspects of confocal Raman microscopy. The role of confocal aperture, the importance of regular alignment and calibration procedures, as well as essential relations between the microscope objective, aperture setting and mapping step are emphasized to understand and successfully operate a Raman microscope. The recent advances in fast Raman imaging technique capable of obtaining both traditional optical and spectrochemical images with a spatial resolution at the diffraction limit of light are outlined.

# Introduction to Raman Spectroscopy

**What are Raman scattering and Raman spectroscopy?**
The interaction of light, a form of electromagnetic radiation, with matter results in the absorption, transmission, reflection, and scattering of light.

The scattering of light by molecules first considered and explained in the works of Rayleigh occurs without changing the frequency of the light––the frequency of the scattered light is equal to the frequency of the incident one. Such scattering is called elastic since the state of the molecule after scattering is the same as before. This is the dominant scattering of light by particles much smaller than the wavelength of the radiation, and this process is called Rayleigh scattering. Rayleigh established that the amount of the scattered light $I$ was inversely proportional to the fourth power of wavelength $\lambda$ of the light for the particles up to about a tenth of the wavelength of light:

$$I \propto \frac{1}{\lambda^4}. \tag{1}$$

The effect of inelastic scattering in liquids and vapors was first experimentally discovered by Chandrasekhara Venkata Raman and Kariamanickam Srinivasa Krishnan and reported in March of 1928 in "Nature".

In this first work, Raman and Krishnan used a simple yet elegant experimental setup in which sunlight was focused by a telescope on scattering materials, thoroughly purified liquids or dust-free gases, and the method of complementary light filters was applied to visually observe "a modified scattered radiation":

Raman and Krishnan examined more than sixty common liquids and vapors and detected the modified scattered radiation with a changed frequency in each of the liquids to a greater or lesser degree.

Sir Chandrasekhara Venkata Raman was awarded the Nobel Prize for Physics in 1930 for his remarkable experimental discovery and proof of the universal character of this effect by investigating a large number of solids and liquids and the first publication of a spectrum of scattered light with changing frequencies. Raman scattering was named after him, and his discovery laid the foundation for the modern use of Raman spectroscopy and Raman microscopy.



**Sir Chandrasekhara Venkata Raman.**

When the light propagates through a matter, the light photons tend not to interact with the molecules of the matter but rather pass through. Only one photon out of about a thousand incident photons is usually scattered by the molecules. Of the scattered photons, an overwhelming majority is elastically scattered, keeping the same energy as the incident photons. Only one out of a million scattered photons changes the energy through an inelastic interaction with the molecules. Therefore, in Raman scattering, the number of photons is about one photon of a billion incident photons.
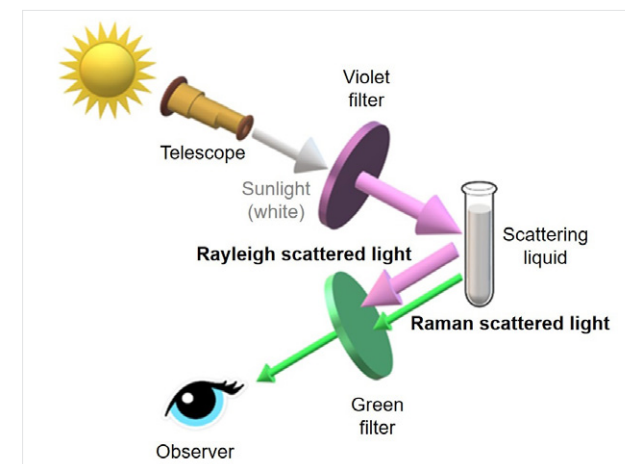
Despite the challenge in the practical detection of the weak Raman effect, the discovery of this physical phenomenon formed the basis of the whole direction of vibrational spectroscopy––Raman spectroscopy.

Vibrational spectroscopy is the most significant portion of molecular spectroscopy because it delivers comprehensive information about the structure and properties of molecules by studying the vibrations and interactions of chemical bonds that associate atoms into molecules. Infrared (IR) and Raman spectroscopies are two major types of vibrational spectroscopy. IR and Raman represent universal tools for the determination and identification of molecular structure in virtually any type of sample and environment. Both methods are complementary, as they provide complete information on molecular vibrations.

In general, a Raman spectrum is composed of a number of spectral lines or bands (the groups of closely spaced spectral lines) displaying their intensity and wavelength position. Each spectral line or band corresponds to a specific molecular bond vibration, including individual bonds such as C-C, C=C, C=O, N-O, C-H, etc., and groups of bonds such as benzene ring breathing mode, polymer chain vibrations, crystal lattice modes, etc.

# Basic Theory and Terminology

**What are Stokes and anti-Stokes Raman scattering?**
According to quantum mechanics, an isolated molecule can only exist in quantized energy states that, in the general case, can be represented by electronic, vibrational and rotational levels of energy. In the quantum-mechanical interpretation, the scattering of a photon by a vibrating molecule is illustrated in Figure 1.

For the sake of simplicity, consider a ground electronic state $E_0$ with only two corresponding vibrational levels of energy denoted by quantum numbers 0 and 1 for the ground and excited level, respectively. The rotational energy levels are ignored since their energy is significantly lower than the energy of vibrations, and the rotation motion is hindered in condensed matter.

The incident photon excites the molecule from an initial energy state to a virtual $E_{virt}$ state, as shown in Figure 1(b). A virtual state is a very short-lived intermediate quantum state that is not defined by a strict molecular energy value. From the virtual state, the molecule instantaneously relaxes back to a vibrational level in the ground $E_0$ electronic state and emits a photon of light. When relaxation occurs, there are three possible situations. First, the molecule is excited from and then relaxes down to the same ground vibrational level 0 and reemits a photon of light with the energy equal to that of the incident photon. As we know, this is an elastic process that corresponds to Rayleigh scattering with the unchanged frequency of the light. The other two situations result in the inelastic scattering of the incident photon that alters its energy. If the molecule is excited by a photon from level 0 and then relaxes to level 1, then the molecule gains energy and reemits a photon of lesser energy (referred to as being "red"-shifted) that corresponds to Stokes Raman scattering. The third possible situation realizes when the molecule is excited from level 1 and then relaxes down to level 0, thus losing its energy and reemitting a photon of light with higher energy than the incident photon.
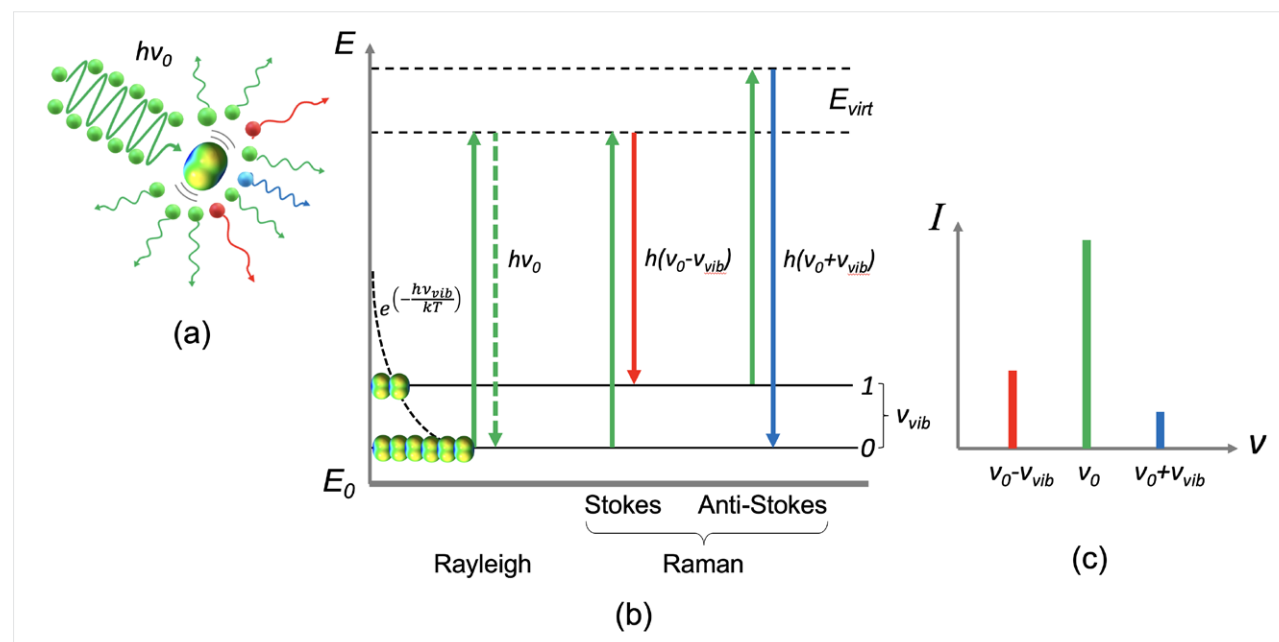


**Figure 1. Schematic representation of quantum-mechanical interpretation of Rayleigh and Raman scattering. (a) The incident photons of light with the energy $h\nu_0$ are scattered off by the vibrating molecule: the green corpuscles symbolize photons with unchanged $h\nu_0$, whereas the red and blue ones imply photons in Stokes and anti-Stokes Raman scattering, respectively. (b) The energy level diagrams illustrate the transition between the vibration levels accompanied by the absorption of an incident photon and emission of a scattered photon: Rayleigh scattering with unchanged energy $h\nu_0$, Stokes Raman scattering with red-shifted photon $h(\nu_0 - \nu_{vib})$ and anti-Stokes Raman scattering with blue-shifted photon $h(\nu_0 + \nu_{vib})$. The left inset sketches the population of the vibrational levels given by the exponential Boltzmann distribution. (c) The illustration of the higher intensity of Stokes Raman (red) scattering with regards to anti-Stokes Raman (blue) scattering as follows from the Boltzmann distribution. *(The figure is reproduced by permission from Alexander Rzhevskii, Modern Raman Microscopy: Technique and Practice, Cambridge Scholars Publishing, 2021, 392.)***

This situation with the "blue"-shifted photon corresponds to anti-Stokes Raman scattering. Thus, Rayleigh ($v_0$), Stokes ($v_S$), and anti-Stokes ($v_{aS}$) spectral components can be observed in scattered light

$$v_0 \,, \quad v_S = v_0 - v_{vib} \,, \quad v_{aS} = v_0 + v_{vib} \,, \tag{2}$$

where $v_0$ is the frequency of incident light and $v_{vib}$ is the frequency of the molecular vibration.

A quantum mechanical approach correctly predicts the difference in intensity between Stokes and anti-Stokes Raman scattering, as illustrated in Figure 1(c). Indeed, the intensity of Raman scattering is proportional to the number of molecules being illuminated. Therefore, the intensity of Stokes Raman scattering is proportional to the number of molecules $N_0$ occupying the ground level 0, whereas the intensity of anti-Stokes Raman is proportional to the number of molecules $N_1$ occupying the excited level 1. At thermal equilibrium, the population of excited vibrational levels decreases exponentially with the difference between the energy of excited and ground levels following the Boltzmann distribution which, in case of $h(v_1 - v_0) = hv_{vib}$ for levels 1 and 0, is given by

$$\frac{N_1}{N_0} = e^{(-\frac{hv_{vib}}{kT})} \,,$$

where $h$ is Planck's constant, $k$ is Boltzmann's constant, and $T$ is the temperature in Kelvin. At room temperature, the ground vibrational energy level is always more populated than the excited one.

Accordingly, there is a much higher probability that photons undergo the Stokes transition, and the intensity ratio of Stokes ($I_S$) to anti-Stokes ($I_{aS}$) Raman scattering depends on the separation between the vibration energy levels and the temperature in accordance with Boltzmann distribution:

$$\frac{I_S}{I_{aS}} \propto e^{(-\frac{hv_{vib}}{kT})} \gg 1 \,. \tag{3}$$

At normal temperatures, this ratio is very large, and anti-Stokes Raman scattering is very weak compared to Stokes Raman scattering. At higher temperatures, the ratio decreases, and anti-Stokes Raman scattering increases noticeably.
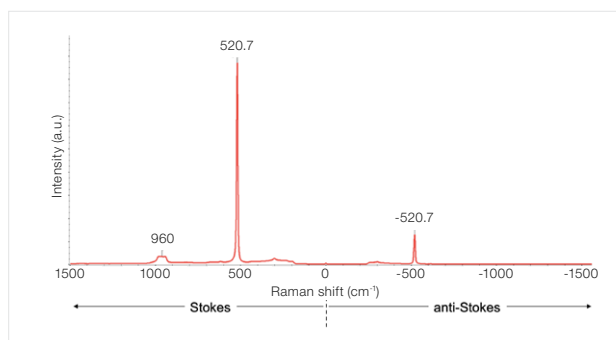


Figure 2. Raman spectrum of a Si wafer in Stokes and anti-Stokes regions. *(The figure is reproduced by permission from Alexander Rzhevskii, Modern Raman Microscopy: Technique and Practice, Cambridge Scholars Publishing, 2021, 392.)*

Figure 2 shows the Raman spectrum of a silicon (Si) wafer in Stokes and anti-Stokes regions. In the Stokes region, the so-called first-order Raman spectrum manifests a strong band at 520.7 cm$^{-1}$ arising from the fundamental transition assigned to the triply degenerate, long-wavelength transverse optical phonon (TO).

The second-order Raman band corresponding to the first overtone is much weaker and is observed at ~ 960 cm$^{-1}$. In the anti-Stokes region, the only first-order band at -520.7 cm$^{-1}$ is evident, whose intensity is about an order of magnitude lower than that of the peak at 520.7 cm$^{-1}$. The example of Si demonstrates that, at ordinary temperatures, the measurement of Raman spectra in the Stokes region has the most practical importance. Indeed, the intensities of spectral bands and, thus, signal-to-noise ratios ($S/N$) in the Stokes region are much higher than those in the anti-Stokes, as follows from (3).

## What is Raman shift?

The frequencies in Raman spectra are usually calculated as a Raman shift, i.e., the difference between the frequencies of excitation light and Raman transitions. Following (2), in Stokes ($v_0 - v_S = v_0 - (v_0 - v_{vib}) = v_{vib}$) and anti-Stokes ($v_0 - v_{aS} = v_0 - (v_0 + v_{vib}) = -v_{vib}$) regions, the vibrational frequencies result in quantities with the sign "plus" and "minus", respectively (see Figure 2). Thus, in the Raman spectrum, the intensities along the ordinate axis are plotted vs. the Raman shift along the abscissa axis, and the shift appears to be independent of the frequency of excitation light. This is why the spectral search against commercial or user-built Raman libraries often used for the identification of unknown compounds can generally be performed for experimental and reference spectra measured with the use of different excitation wavelengths.

## What does Raman intensity depend on?

As follows from (1), $I \propto (v_0)^4$. It can be shown that the intensity of Stokes Raman component scattered by $N$ molecules of a sample can be written as

$$I_S \propto I_0 N (v_0 - v_{vib})^4 \left(\frac{\partial \alpha}{\partial q}\right)^2,$$

(4)

where $I_0$ and $v_0$ are the intensity and the frequency of the excitation light, respectively, and the derivative $(\partial \alpha / \partial q)$ is the rate of change of the polarizability $\alpha$ of a molecule or chemical bond upon the displacement of nuclei $q$ from the equilibrium position. This dependence can be presented in the form to some extent analogous to the Lambert-Beer law that establishes the relationship between the sample absorbance $A$, the extinction coefficient (absorptivity) $\varepsilon$, the concentration of the molecules $C$, and the pathlength that light travels through the sample $d$ in IR spectroscopy: $A=\varepsilon Cd$. Thus, the relationship (4) for Raman scattering can be expressed as

$$I_R = K I_0 \sigma C V,$$

(5)

where $K$ is a parameter mostly determined by experimental conditions of spectral measurement, $C$ is the concentration of the molecules in the sample, and $V$ is the sampling volume, i.e., the volume from which the scattered light is collected and measured. However, in contrast to the Lambert-Beer law, the intensities of Raman bands linearly depend on the intensity $I_0$ of excitation light. The coefficient $\sigma$ defined as

$$\sigma \propto (v_0 - v_{vib})^4 \left(\frac{\partial \alpha}{\partial q}\right)^2$$

(6)

characterizes the ability of a molecule or chemical bond to scatter light at a given frequency of vibration $v_{vib}$ and is called a Raman scattering cross-section.

The absorptivity $\varepsilon$ and Raman cross-section $\sigma$ play a somewhat similar role in both methods of vibrational spectroscopy. These coefficients are a measure of the probability of a specific transition to occur and characterize the intrinsic properties of molecules or chemical bonds to absorb and scatter light. However, the Raman cross-section $\sigma$ strongly depends on the excitation frequency being proportional to its fourth power. That is, for a given sample, replacing a 1064 nm laser with a 532 nm laser (both of which are popular choices for Raman spectroscopy) increases the scattering cross-section by a factor of 16 (see Figure 3). Thus, an important outcome of expressions (5) and (6) is that the intensities of Raman bands can be increased by increasing the intensity $I_0$ and/or the frequency $v_0$ of excitation light. Nevertheless, as in IR, the intensities of spectral bands are proportional to the concentration of an analyte $C$, making Raman spectroscopy well suitable for quantitative analysis.
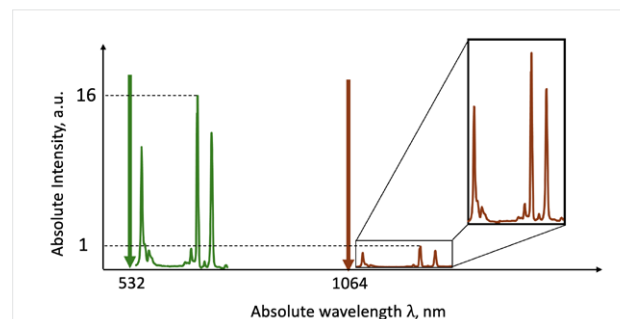


Figure 3. The difference in the absolute intensity of spectral bands in the Raman spectrum of Sulphur obtained with 532 and 1064 nm excitation wavelengths. Note that the relative intensities of the Raman bands remain unchanged and do not depend on the excitation wavelength.

## What are the selection rules in IR and Raman spectroscopy?

A simple classical approach that takes the changes in the dipole moment and the polarizability during the molecular vibration into consideration can be used to explain if the vibration results in a corresponding IR or/and Raman spectral band. The dipole moment arises from the difference in electronegativity of atoms composing chemical bonds and due to non-uniform distributions of positive and negative charges on the various atoms in a molecule. The magnitude of the dipole moment of an individual chemical bond composed of atoms that have different electronegativity is given by

$$\mu = Ql,$$

where $Q$ is the charge and $l$ is the distance between the atoms. Thus, the dipole moment is a measure of the charge asymmetry of a molecule. The total dipole moment of a polyatomic molecule is a vector sum of the individual dipole moments of chemical bonds. The dipole moment oscillates during molecular vibration with the frequency of the vibration $v_{vib}$:

$$\mu = \mu_0 \cos(2\pi v_{vib} t),$$

where $\mu_0$ is the permanent dipole moment in the equilibrium state of the molecule and $t$ is time.

The classical electromagnetic theory requires that for a molecule to absorb the light, the change in the dipole moment with respect to displacement during the vibration (the first derivative) must be non-zero:

$$\left(\frac{\partial \mu}{\partial q}\right)_0 \neq 0 , \tag{7}$$

and the corresponding vibration is said to be IR-active.

The oscillating electric field of the light wave perturbs the cloud of electrons surrounding the nuclei and displaces the center of the electron cloud relative to the center of the nuclei. The displacement results in an induced dipole moment $p$:

$$p = \alpha E , $$

where $\alpha$ is the polarizability of the molecule and $E$ is the electric field of the light wave with the amplitude $E_0$ that oscillates with time $t$ as a cosine function

$$E = E_0 \cos(2\pi \nu_0 t) . \tag{8}$$

Thus, the oscillation of the induced dipole moment $p$ occurs with the frequency $\nu_0$ of the light wave:

$$p = \alpha E_0 \cos(2\pi \nu_0 t) . \tag{9}$$

The interaction of light with a molecule leads to the appearance of an induced dipole moment, even if there may be no permanent dipole moment. An important consequence of equations (8) and (9) is that for Raman scattering to occur, the vibration that changes the polarizability $\alpha$ with the displacement of nuclei $q$ must be non-zero:

$$\left(\frac{\partial \alpha}{\partial q}\right)_0 \neq 0 , \tag{10}$$

and the vibration is said to be Raman-active. By contrast, if the molecular vibration does not cause a variation in the polarizability $\alpha$, then there is no amplitude modulation of the dipole moment, and there is no Raman Stokes and anti-Stokes radiation. Such vibration is called Raman-inactive.

The necessary conditions for an active vibration expressed by formulas (7) and (10) are often termed the gross or major selection rules, respectively, for IR absorption and Raman scattering. In a polyatomic molecule, the vibrations that bring on a net change in a dipole moment are IR-active, and those that induce polarizability changes are Raman-active. Obviously, some vibrations can be both Raman- and IR-active.

### What is the ellipsoid of polarizability?

The polarizability $\alpha$ of the molecule is an important parameter in the classical theoretical consideration of the Raman effect. Polarizability can be described as a measure of the deformability of the electron cloud in the molecule or, in other words, how easily the electron cloud can be distorted by the electric field of the light wave interacting with the molecule. The polarizability $\alpha$ is not constant because the vibrations of atoms in the molecule can cause it to alter. The polarizability of a molecule can be represented in the form of an ellipsoid called the ellipsoid of polarizability that helps to visualize how the polarizability of a molecule changes during its vibrations and to figure out whether or not a given vibration is Raman-active.
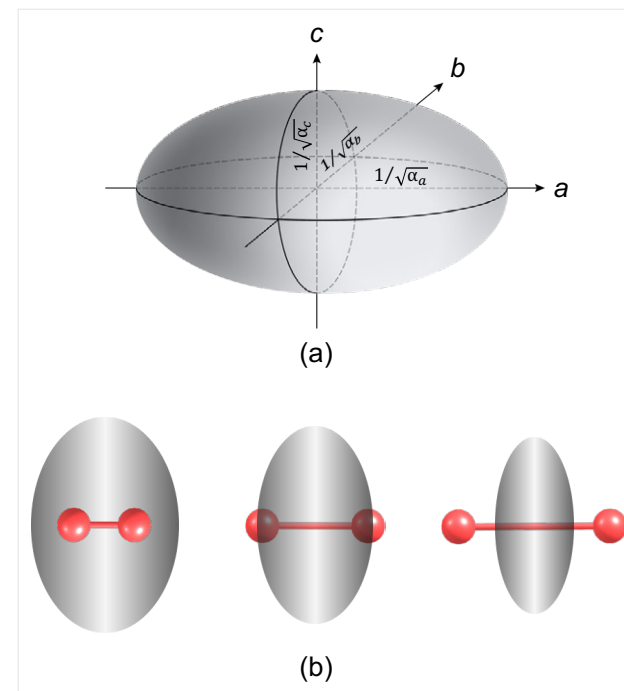


(a)

(b)

Figure 4. The ellipsoid of polarizability. (a) Half the lengths of the principal axes are inversely proportional to the square roots of the components of the polarizability in the orthogonal axes a, b and c. (b) The change of the ellipsoid of polarizability for the homonuclear diatomic molecule $O_2$ upon its vibration. *(The figure is reproduced by permission from Alexander Rzhevskii, Modern Raman Microscopy: Technique and Practice, Cambridge Scholars Publishing, 2021, 392.)*

The ellipsoid of polarizability is shown in Figure 4(a). The axes $a$, $b$ and $c$ are termed "principal" axes that can often be chosen so that they are related to the symmetry axes of a molecule. Note that the axes of the ellipsoid are inversely proportional to the square roots of the components $\alpha_a$, $\alpha_b$ and $\alpha_c$ of the polarizability in the orthogonal axes $a$, $b$ and $c$. Since the electrons are more polarizable in the direction of a chemical bond (a larger $\alpha$), the shortest axes of the polarizability ellipsoid correspond to the directions of the easiest polarization, as shown in Figure 4(b) for a homonuclear diatomic molecule.

A vibration is Raman-active if the size, shape or orientation of the polarizability ellipsoid changes during the vibration. In a homonuclear diatomic molecule, such as $O_2$, $H_2$ or $N_2$, there is no permanent dipole moment in their equilibrium states. The vibration of the only truly covalent nonpolar bond does not change the dipole moment such that the derivative of the dipole moment (7) is zero, and the vibrations of these molecules are not IR-active. However, the polarizability of the molecules changes with the nuclear displacement, and the vibration results in a non-zero derivative in (10). As shown for the $O_2$ molecule, the polarizability ellipsoid noticeably changes alongside the bond, and, therefore, the vibration is Raman-active. The vibrational bands of $O_2$ and $N_2$ can be correspondingly observed at about 1556 and 2329 cm$^{-1}$ in the Raman spectrum of ambient air.

### What is Raman polarization?

In modern Raman instruments, the lasers used for the excitation of Raman scattering are usually linearly polarized by design. It means that the electric field vector of the light wave is oriented along a single axis perpendicular to the direction of the light beam generated by the laser. When exposed to linearly polarized light, a sample may interact differently with light resulting in dissimilar Raman spectra depending on how the sample is oriented relative to the direction of the polarization axis. However, not all materials are sensitive to the orientation of polarized light. The term isotropic means the properties of the sample (e.g., its Raman spectrum) are not sensitive to sample orientation. Examples include liquids, powders, and randomly oriented polymers. While these samples are not sensitive to orientation, they may still interact with polarized light and cause the polarization of the scattered Raman beam to be changed relative to the incident laser polarization. In contrast, samples such as solid or liquid crystals, carbon nanomaterials, strained polymer films and fibers are typically very sensitive to sample orientation and are called anisotropic. Oriented or anisotropic samples have an axis of symmetry or an optical axis. The orientation of this axis relative to the incident laser polarization can result in quite different spectra.

Hence, Raman spectra measured using the naturally polarized light may not be well reproducible if the relative orientation of the anisotropic samples and the direction of the laser polarization is not taken into consideration. For this reason, the laser excitation beam is purposely depolarized in general-purpose instruments to ensure consistent results regardless of the sample orientation. The Raman spectra obtained using the depolarized laser excitation are referred to as depolarized Raman spectra. Advanced Raman instruments can be configured to perform both depolarized and polarized Raman measurements.

The polarization of the laser beam can be achieved using a polarizer or polarization filter. The polarizer is oriented accordingly to obtain the required direction of polarization of the laser beam. The scattered light may consist of the components with the directions of polarization parallel and perpendicular to the electric field vector in the incident light. The ratio of the intensities of the perpendicular to the parallel component is called the depolarization ratio $\rho$:

$$\rho = \frac{I_\perp}{I_\parallel}.$$

This ratio represents an important value measured in Raman spectroscopy because it depends on the symmetry of the molecule and a given molecular vibrational. A Raman spectral band with a depolarization ratio in the range of $0 \leq \rho \leq \frac{3}{4}$ is called a polarized band, and a band with a depolarization ratio $\rho \geq \frac{3}{4}$ is called a depolarized band.

In a typical polarization experiment, a Raman spectrum is collected with the light linearly polarized in one direction, and then another spectrum is collected with the light polarized perpendicular to the first direction. Normally, the polarization experiment is performed without a polarization analyzer so that the scattered light of both polarizations is measured at its maximum intensity. However, polarizers and analyzers are the parts of Raman polarization optics in which the analyzer acts as a second polarizer. The main functional purpose of the analyzer is that it can be used to accurately check whether the polarization of the light has been changed after the interaction with a sample. The analyzer can usually be set to either parallel or perpendicular to the polarization of the excitation light, but the intensity of Raman scattering decreases especially noticeably if the analyzer and polarizer are oriented orthogonally (crossed). Nevertheless, there are situations in which the use of the analyzer can be helpful in the characterization of materials and assignment of the spectral bands in their Raman spectra.

When making polarization measurements, it is important to keep track of the directions of polarization, i.e., the orientation of the polarizer and analyzer, so that the results can be unambiguously interpreted. In polarization-dependent Raman spectroscopy, it is usual to designate the directions of incident and collected light and the directions of polarization using the so-called Porto notation.

Porto notation describes the position of a sample with respect to the orientations of the polarizer and analyzer. The designation consists of four terms written in the form of

$$a(bc)d$$

and defined as follows:

a. direction of propagation of the incident laser beam

b. direction of polarization of the incident laser beam

c. direction of polarization of scattered light

d. direction of observations of scattered light

In the majority of modern Raman instruments, including DXR series of Raman spectrometers and microscopes, the so-called 180-degree backscattering sampling configuration is implemented by design. It means that the excitation laser beam propagates along a certain axis, and the Raman scattering is collected along the same axis but in the opposite direction. By convention, the $Z$-axis of the Cartesian coordinate system is chosen to be vertical. The convention is also to use an overbar on the $Z$-axis notation to designate the opposite direction $\overline{Z}$. Thus, as follows from Figure 5, if the excitation laser beam incidents along the $Z$-axis, there are only four principal polarization orientations that can be analyzed with a Raman instrument:

- $Z(XX)\overline{Z}$ - laser is polarized parallel to an X-axis; analyzer is set to pass the light polarized in X-axis;

- $Z(YY)\overline{Z}$ - laser is polarized parallel to a Y-axis; analyzer is set to pass the light polarized in Y-axis;

- $Z(XY)\overline{Z}$ - laser is polarized parallel to an X-axis; analyzer is set to pass the light polarized in Y-axis (polarized and analyzer are crossed);

- $Z(YX)\overline{Z}$ - laser is polarized parallel to a Y-axis; analyzer is set to pass the light polarized in X-axis (polarized and analyzer are crossed).
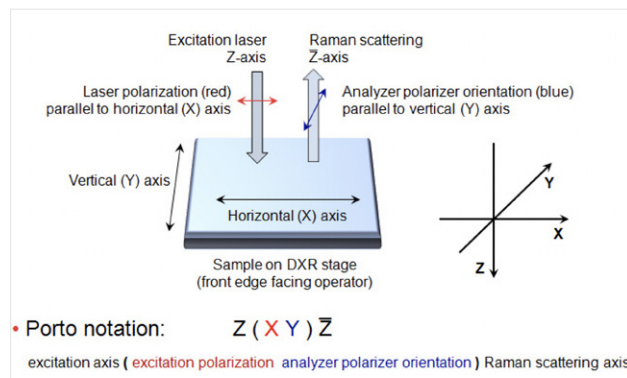


Figure 5. Orientation polarization axes at the sample in DXR2(3) Raman microscope and the corresponding Porto notation.

For an anisotropic sample, it is recommended to make measurements for all four positions of the polarizer and analyzer relative to the sample's orientation to describe the sample by means of polarization-dependent Raman spectroscopy. Polarized Raman with angle resolution offered in DXR2 and DXR3 series of Raman microscopes, when the analyzer can be set between 0 and 90 degrees with an increment of one degree, provides additional flexibility in Raman polarization experiments. It is also a good practice to measure the spectrum with the non-polarized incident laser beam to characterize the sample as completely as possible.

Historically, polarization-dependent Raman spectroscopy has helped to determine the symmetry of the vibrations and correctly assign the observed Raman bands. Classic examples of the polarized Raman spectra of cyclohexane and carbon tetrachloride can be found in many textbooks and original articles. In general, polarization-dependent Raman spectroscopy provides information about preferentially oriented molecules or materials. For example, a drug may crystallize in different polymorphic forms which have identical spectra when measured with depolarized light. When examined under linearly polarized light, the drug spectra may change providing confirmation of a specific crystalline structure. Polarization measurements are also commonly used to reveal strain in materials such as stretched polymer films, doped silicon structures or cast materials.

### What are the benefits of Raman spectroscopy?

As mentioned above, Raman spectroscopy provides chemical and structural information complementary to Fourier-transform Infrared Spectroscopy (FTIR). In general, chemical compounds manifest distinctive spectral bands in their Raman and FTIR spectra, but they may not coincide due to different selection rules. Which technique provides better results depends on the samples under study, the concentration of analytes, the surrounding matrix or solution, the presence of impurities, the desired sampling method, and whether the sample is under temperature or pressure. For many applications, Raman spectroscopy offers indisputable advantages; the major ones are as follows:

1. No sample preparation is required, or the sample preparation is rather trivial. In contrast to FTIR, which often requires dissolution, diluting or pressing samples into pellets, no physical or chemical treatment of the sample is typically necessary for Raman measurements. In principle, if a sample under study fits into the sample compartment of a Raman instrument, the Raman spectrum of the sample can be obtained.

2. The technique is nondestructive and saves the sample integrity, provided that careful control of the laser radiation density is carried out to ensure that there is no laser-induced modification to the sample. Then, after the Raman measurements, the sample can be treated and analyzed by other methods. The nondestructive aspect is of paramount importance for forensic analyses where the samples collected during an investigation should be kept intact.

3. The non-contact method of examination of samples by light provides safe procedures for both samples and operators. On the one hand, the procedure ensures that no contamination is introduced into the sample. On the other, hazardous, toxic or unstable to air or moisture samples can be measured through a protective sampling insertion or placed in sealed glass containers. Samples can be analyzed through transparent windows, cuvettes, vials, bottles or translucent polymer packaging.

4. Remote analysis can be conveniently realized in Raman spectrometers. Fiberoptic probes transmit laser light and collect Raman scattering over long distances, up to hundreds of meters away from the mainframe of the Raman instrument.

5. The nondestructive, noninvasive and non-contact nature of the Raman measurement makes it very suitable for *in situ*, *in vitro* and *in vivo* analysis. It can be used to monitor chemical reactions *in situ* within a reaction chamber, often at cryogenic or very high temperatures and pressures, including the identification and quantitation of combustion products in flames and plasmas. Raman spectroscopy can be used for *in vitro* and *in vivo* characterization of the chemical and morphologic structure of biological cells, tissue and microorganisms.

6. Since water is a weak Raman scatter and does not manifest much in Raman spectra, Raman spectroscopy is ideal for the study of analytes, e.g., biological compounds, in aqueous solutions. There is no need for time-consuming sample extraction or drying that may also alter the chemistry of the sample. This is a significant advantage over FTIR spectroscopy, which capabilities are limited by the strong absorption of water when the analysis of aqueous solutions is required.

7. Raman spectroscopy is applicable to a wide range of substances and materials. Raman spectra of liquids, solids, gases (even those composed of homonuclear molecules), vapors and aerosols can be obtained. The only exception is pure metals and alloys, which just reflect light. However, metal oxides, carbides and nitrides are Raman-active. Samples can be in the form of a solution, slurry, gel, powder, chunk, crystal, wafer, film or fiber with various sizes, shapes and thicknesses.

8. During Raman spectral measurements, the full spectral region of fundamental vibrations, usually from 50 to 3500 cm$^{-1}$, can be recorded in a single exposure. Thus, Raman spectra are appropriate for the characterization of organic and inorganic compounds, such as those used in polymer composites. In contrast, FTIR instruments typically require reconfiguration (a change of beamsplitters, detectors or sources) in order to cover the spectral region below 400 cm$^{-1}$.

9. Beyond general material characterization and identification, Raman spectroscopy also provides information on more subtle chemical effects, such as the extent of crystallinity, polymorphism, phase transformation, strain in materials and protein secondary structure.

10. Often, due to the higher likelihood of the presence of the Raman bands that are well resolved and do not overlap with their neighbors, Raman spectra are better suitable for material identification by a spectral library search.

11. Both Raman and FTIR methods can be used with the microscopic technique. However, combining a Raman spectrometer with a microscope results in one of the major advantages over FTIR: an order of magnitude better spatial resolution. Spatial resolution is improved because Raman spectroscopy uses an excitation wavelength in the visible region of the spectrum, whereas FTIR uses longer wavelengths in the infrared region. The shorter excitation wavelengths of visible light result in a smaller diffraction limit and can, therefore, be focused onto a smaller spot on the sample than the longer wavelengths of infrared light. Raman microscopy is currently capable of probing objects as small as about 0.5 μm, whereas an FTIR microscope can resolve structures of 5–10 μm at best. Thus, individual particles, defects, trace amounts of substances, biological cells and microorganisms can be analyzed by Raman microscopy on a sub-micron level.

12. A confocal analysis is another unique advantage of Raman microscopy. A confocal Raman microscope allows the measurement of a minuscule discrete volume in a transparent sample and, thus, can provide the analysis at different depths and even 3D spectrochemical rendering without physical slicing of the sample. The confocal capability is particularly useful for the nondestructive analysis of layered samples (e.g., multi-layered polymer films), volume inclusions and defects (in glass materials, plastics or minerals), semiconductor thin films, polymer composites, and many others.

In fairness, it should be noted that Raman spectroscopy also has known disadvantages. The major one is certainly the fluorescence interference that is considered below. Also, the laser power aimed at the sample needs to be thoroughly controlled to avoid local heating or photodecomposition, especially in resonance Raman experiments where the laser frequency is intentionally tuned into the absorption band of the compound under study.

## What is fluorescence, and how does it interfere with Raman spectra?

As it is known, vibrational spectra are observed as a result of transitions between quantized energy levels of molecules. Figure 6 shows the transitions in the cases of IR absorption, Raman scattering and fluorescence, along with the approximate quantum yields (QY) of the corresponding processes. QY is defined as the number of times the acts of photon absorption, scattering or reemission occur divided by the number of incident photons in IR absorption, Raman scattering or fluorescence, respectively. For the sake of simplicity, only two vibrational levels, the ground $v_0$ and the first excited $v_1$, are shown for the ground $E_0$ and the first excited $E_1$ electronic states, and arrows indicate transitions between these levels. $E_{virt}$ denotes the short-lived intermediate quantum state participating in Raman scattering. The Raman transitions are shown for Stokes scattering only. Typical excitation frequencies in NIR, visible and UV regions are marked in the energy (eV) and wavelength (nm) vertical axes.
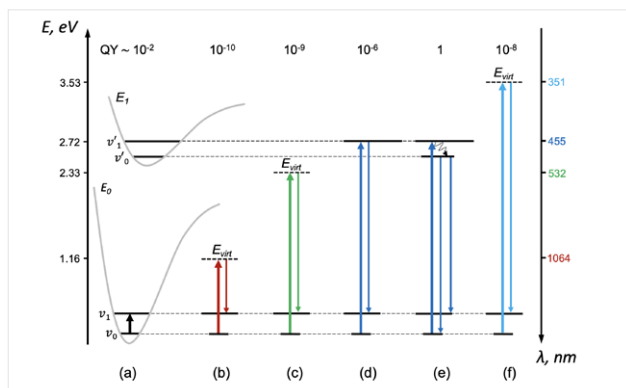


Figure 6. The transitions between the vibrational energy levels of a diatomic molecule as the excitation energy increases from left to right and the approximate quantum yields (QY) of the corresponding processes: (a) IR absorption; (b) Raman with excitation in the near-infrared region (NIR-Raman); (c) Raman with excitation in the visible region (Vis-Raman); (d) resonance Raman; (e) fluorescence; and (f) Raman with excitation in the UV region (UV-Raman). *(The figure is reproduced by permission from Alexander Rzhevskii, Modern Raman Microscopy: Technique and Practice, Cambridge Scholars Publishing, 2021, 392.)*

As mentioned above, the low quantum yield (QY) of the Raman effect is the major challenge in the practical detection of Raman scattering. Another challenge to Raman scattering comes from fluorescence emission that has a similar origin but a much higher QY. Fluorescence may overwhelm or mask the relatively weak Raman signal, and the problem of circumventing fluorescence is of great importance in practical Raman spectroscopy.

For the process of fluorescence to arise, a molecule must first absorb a photon with enough energy (typically in the visible or ultraviolet range of the optical spectrum) to excite it from the ground to a higher electronic energy state. Then, the molecule quickly relaxes back down to the more stable ground state, releasing the excess energy. The release of the extra energy often occurs through a non-radial transition to a lower vibrational level of the same electronic state, followed by the spontaneous reemission of a photon having less energy than the absorbed photon. The so-called non-radial decay is shown by the wavy arrow between $v'_1$ and $v'_0$ vibrational levels in Figure 6(e).

Fluorescence originates from fluorophores, the chemical compounds whose molecules typically contain several conjugated aromatic groups or heterocyclic systems with π-bonds. These parts of the molecules are called chromophores, and they are responsible for the colors of the chemical compounds.

Aromatic hydrocarbons, such as fluorescein, phenolphthalein, naphthalene, anthracene and perylene, generate a strong fluorescence upon excitation with visible light. The intrinsic fluorescence of biological tissues is often related to the presence of proteins, especially hemoglobin. In spectroscopy, this type of fluorescence is called autofluorescence. However, fluorescence may also originate from molecules of impurities of different nature and trace elements in the materials under study.

In many practical cases, fluorescence background is a major problem when measuring Raman spectra. Indeed, the intensity of the fluorescence band is proportional to the amount of the absorbed light, and the maximum possible QY of fluorescence is 1.0 (100%) when each photon absorbed results in a photon emitted. Fluorophores that provide QY of 0.1 are considered to be strong fluorescent compounds. Thus, the fluorescence background can be up to $10^{10}$ times more intense than Raman scattering. Even weak fluorescence from the analyte or impurities in the sample is often much stronger than the Raman scattering and, therefore, can obscure the Raman bands.

As it follows from Figure 6, fluorescence only occurs if a molecule is excited up to a higher electronic state. Fluorescence can by significantly reduced by using longer excitation wavelengths, such as the visible 785 nm or near-infrared 830 and 1064 nm, where the photon does not have enough energy to excite most of the molecules to higher electronic states. Another way to minimize fluorescence is photobleaching by prolonged sample exposure to excitation light.

# Raman Spectrometer

## What are the major components of the Raman instrument?

Raman instruments are all built around the principles developed by the persons who first discovered and observed Raman scattering. Soon after the pioneering experiment with sunlight and light filters, C.V. Raman used a mercury arc lamp as the excitation source and a quartz spectrograph that allowed the first Raman spectra to be photographed.

A modern Raman instrument is an integrated system that generally combines an excitation source, a spectrometer, a sampling compartment or accessory, and a controlling computer with the software for the acquisition and numerical processing of spectral data. Many different configurations of Raman instruments exist depending on the application, and these configurations may require additional parts and optical components. For example, in a Raman microscope, a laser excitation source and a spectrometer are combined with an optical (light) microscope for non-destructive spectrochemical analysis of a variety of materials and objects at the microscopic level.

The common layout of a dispersive Raman microscope with all its major parts and optical components is depicted in Figure 7.
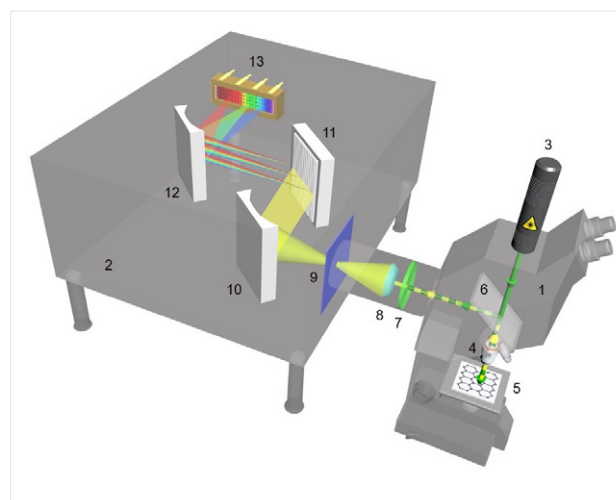


Figure 7: Schematic diagram of a dispersive Raman microscope: 1 – optical microscope; 2 – spectrograph; 3 – laser source; 4 – microscope objective; 5 – sampling stage with a sample; 6 – beamsplitter or dichroic mirror; 7 – Rayleigh filter; 8 – microscope-to-spectrograph coupling optics; 9 – spectrograph entrance aperture; 10 – collimating mirror; 11 – diffraction grating; 12 – focusing mirror; 13 – array detector. *(The figure is reproduced by permission from Alexander Rzhevskii, Modern Raman Microscopy: Technique and Practice, Cambridge Scholars Publishing, 2021, 392.)*

An optical microscope (1) is used to observe a sample and focus the laser beam on it. In the Raman microscope, the excitation of the sample and the collection of scattered light are performed in a so-called back-scattering or 180-degree configuration. The laser (3) emits excitation light (the green beam) that is focused by the microscope objective (4) onto the sample placed on the sample stage (5). The light is then scattered by the sample, collected by the same objective and directed through the plate beamsplitter (6) into the spectrograph (2). Thus, after being scattered by the sample and collected by the objective, the Raman and Rayleigh components of scattered light share a common path. These components are shown by the yellow and green dotted beams, respectively. The Rayleigh scattered component is then blocked by the Rayleigh rejection filter (7). An optical interface (optical coupling) between the microscope and spectrometer (8) is used to transfer Raman scattering to the spectrograph. Raman scattering passes through the spectrograph's entrance aperture (a pinhole as shown or a slit) (9) and is collected by the collimating mirror (10). The mirror directs the collimated beam onto the diffraction grating (11). The grating decomposes Raman scattering into its constituent spectral components, which are focused by a second mirror (12) onto the multi-element array detector (13).

## How to select the appropriate excitation (laser) wavelength?

Interest in Raman spectroscopy increased dramatically in the late 1960s after the invention and commercialization of lasers as new monochromatic and powerful sources of excitation light. Lasers have completely replaced the mercury lamps that were used as light sources in the early days.

One of the main advantages of Raman spectroscopy is that the appearance of the measured spectrum is independent of the excitation wavelength (see Figure 3). Nevertheless, the appropriate choice of laser excitation wavelengths is necessary to obtain the most informative Raman spectrum of a given sample.

As we know from equation (1), the scattering intensity is inversely proportional to the fourth power of the excitation wavelength, $1/\lambda^4$. Therefore, Raman spectroscopists prefer shorter laser wavelengths, such as blue 488 nm, green 514 and 532 nm or red 633 nm, to obtain a stronger Raman signal and, respectively, a better signal-to-noise ratio ($S/N$) in the spectrum provided that all the other experimental conditions are equal. Blue and green wavelengths are typically reasonably suitable for transparent liquids and polymers, non-colored inorganic materials and some resonance Raman experiments. However, as the Raman effect is an extremely weak phenomenon, a Raman signal in the visible optical range can easily be overwhelmed by autofluorescence from an analyte or even fluorescence from trace impurities in the sample under study.

For measurements of highly fluorescent materials, it is common to use NIR laser excitation with a 1064 nm wavelength. Although 1064 nm excitation ensures virtually fluorescence-free Raman spectra, it results in a theoretical decrease in scattering efficiency by a factor of 16 compared to the green 532 nm wavelength.

Excitation in the UV spectral region is attractive for resonance Raman spectroscopy on biomolecules, such as proteins, DNA and RNA. It also provides a unique opportunity to avoid both the fluorescence and interference of thermal emission at high temperatures in studying catalysts and catalytic processes *in situ*. Moreover, because of the $1/\lambda^4$ dependence, Raman scattering efficiency is higher in the UV region. Nevertheless, UV excitations in Raman spectroscopy need to be applied with care since thermal decomposition or other laser-induced modifications of samples are possible.

It is well recognized that the best trade-off between Raman scattering efficiency, fluorescence avoidance, laser-induced effects and compatibility with the detector's sensitivity can be achieved with the dark red 785 nm laser wavelength. It should be noted that 785 nm excitation causes a significant fluorescence in glass commonly used for laboratory glassware. A broad fluorescence band centered at about 1385 cm$^{-1}$ originates from rare earth elements and certain impurities in the glass matrices. Therefore, it is recommended to avoid cuvettes, vials, microscope slides, coverslips and substrates made of glass when using 785 nm excitation, as the fluorescence may significantly distort the measured Raman spectrum.

Also, a combination of a 785 nm laser with a back-illuminated CCD detector in the Raman spectrograph, as explained below, may result in an unwanted interference pattern in the Raman spectrum.

Depending on the application and the material under investigation, using several excitation wavelengths and switching between different wavelengths in a Raman instrument are considered to be a substantial advantage. Figure 8(a) provides an example of the application of different excitation wavelengths to characterize the diameter distribution of single-wall carbon nanotubes (SWCNT) in a mixture using the position and intensity of their Raman radial breathing modes (RBMs). Further analyzing their Raman spectra can predict the chirality and semiconducting or metallic behavior of the SWCNTs. Figure 8(b) shows the Raman spectra of graphene grown by the chemical vapor deposition (CVD) process on a copper foil. Note that green 532 nm laser excitation generates a significant baseline humpback due to the fluorescence of the copper substrate, whereas blue 455 nm excitation avoids fluorescence resulting in a flat baseline with well observable Raman bands.
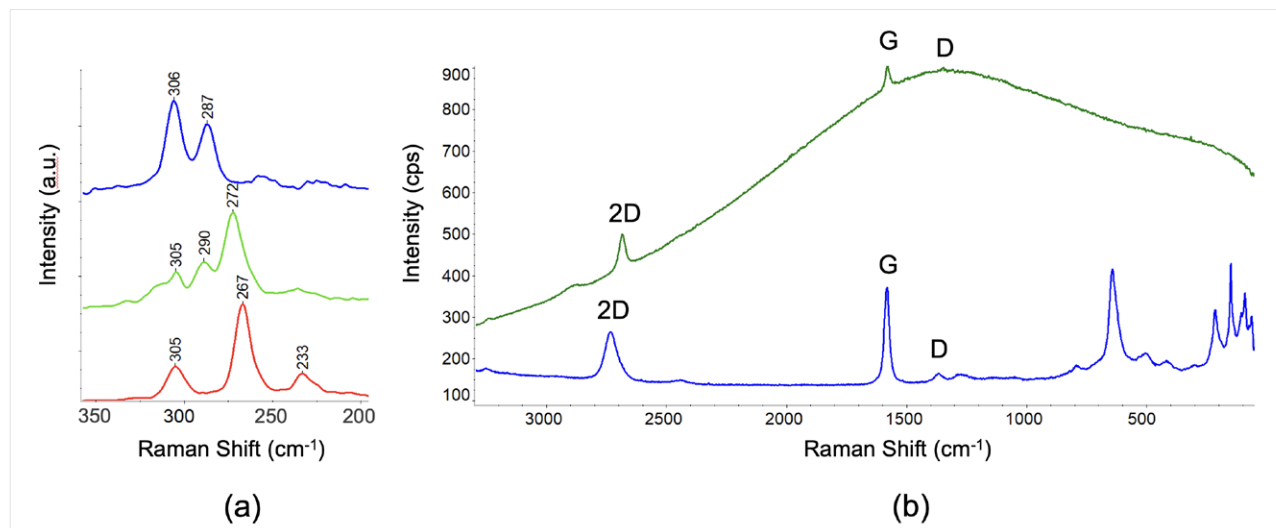
Figure 8: The influence of different excitation wavelengths on Raman spectra. (a) Raman spectra of a mixture of SWCNTs in the region of manifestation of RBMs measured with 455 (blue), 532 (green) and 633 (red) nm excitation wavelengths (the spectra are offset for clarity). (b) Raman spectra of multi-layered graphene on a copper foil measured using 532 (green) and 455 (blue) nm wavelengths. The principal bands of graphene are marked as G, D and 2D. The bands in the region below 800 cm-1 belong to copper oxide formed on the surface of the copper foil.



Figure 9: The effect of increasing 532 nm laser power on $C_{60}$.

In practice, when working with various applications and materials, Raman spectroscopists always want access to as many excitation wavelengths as possible to perform Raman experiments successfully and optimally. Therefore, flexibility and optimization of Raman experiments are achieved in high-end Raman spectrometers and microscopes with multiple lasers, interchangeable Rayleigh filters and diffraction gratings.

DXR Raman instruments can be equipped with 455, 532, 633 and 785 nm laser sources.

## Why is fine control of laser power at the sample important?

Since a laser beam creates a very high density of light power in focus, it is important to protect sensitive samples from any thermal or photochemical damage. For some materials, it is possible to damage or alter the sample with laser radiation. This damage can be very obvious in extreme cases where the laser radiation burns a hole in the sample. In other cases, the damage can be more subtle, and if care has not been taken to avoid damaging the sample, it may result in Raman spectra that do not represent the actual sample. Such spectral data could easily be misinterpreted. Figure 9 provides an example of one such situation with a sample of $C_{60}$ fullerene. Here we can see that the $C_{60}$ begins to breakdown into other structures, probably amorphous carbon, with as little as 0.5 mW of the 532 nm laser power at the sample.

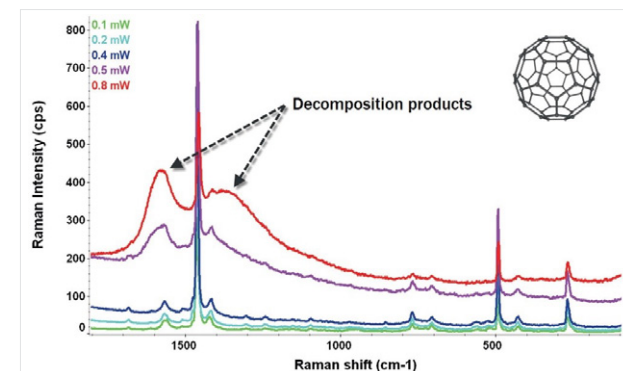DXR Raman instruments are equipped with variable neutral density filters set at the laser output. The continuously variable opacity of the filters allows accurate and reproducible light power with 0.1 mW increments to be delivered to the sample. It may be of critical importance when light-sensitive samples such as biological cells and tissues, carbon nanomaterials, and many others are being measured.

## How does spectrograph work?

An optical spectrometer performs a spectral (harmonic) analysis of light. This analysis is most often carried out using a dispersing element (usually, a diffraction grating), thereby deflecting the light rays of different wavelengths at different angles. A spectrometer with a dispersing element is called dispersive, while a spectrometer that performs spectral analysis based on the principle of optical interferometry, such as the Michelson interferometer in the FT-Raman instrument, is called non-dispersive.

A typical dispersive spectrometer consists of five basic components: 1) an entrance aperture, 2) collimating optics, 3) a diffraction grating, 4) focusing optics, and 5) a detector.

The most widely used spectrograph configuration for Raman spectroscopy is based on the Czerny–Turner design outlined in Figure 10(a). The entrance aperture may be a slit, a pinhole or the output end of an optical fiber, and the spectrum can be essentially regarded as a discrete number of monochromatic images of the entrance aperture in the focal plane of the spectrometer. However, as will be considered below, the aperture confines an element of the sample from which the spectrum is measured. Thus, the aperture performs two main functions: it provides both the necessary spectral and spatial resolution.

The Czerny–Turner spectrograph employs concave collimating and focusing mirrors and a planar reflective diffraction grating. The collimating mirror collects the light diverging from the input aperture, forms a collimated beam of light and directs it to the diffraction grating. The collimating optics ensure that the full area of the diffraction grating is illuminated, which is necessary for the optimal operation of the grating. The diffraction grating separates the light rays in space as a function of wavelength so that each constituent wavelength component is deflected under a certain angle, but all rays of the same wavelength travel under the same angle. The dispersed rays are then collected by the focusing mirror, which forms an image of the entrance aperture by focusing the light rays of different wavelengths at the exit focal plane. The detector placed in the exit focal plane generates an analog electrical signal proportional to the intensity of the light that hits the detector. If the rays of different wavelengths are scanned over the detector through an exit slit sequentially by rotating the diffraction grating, then the instrument operates as a monochromator.
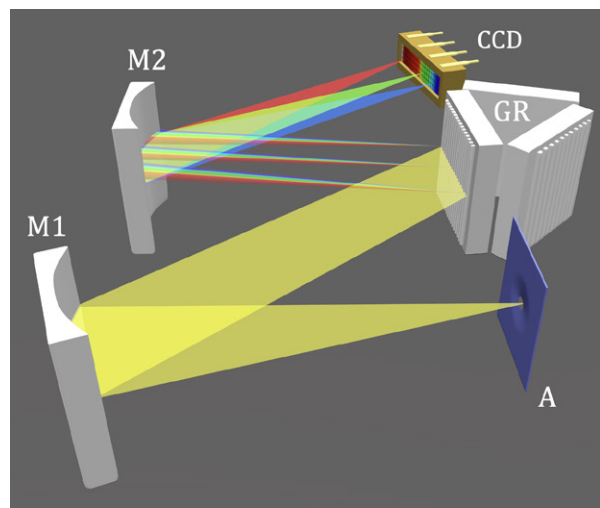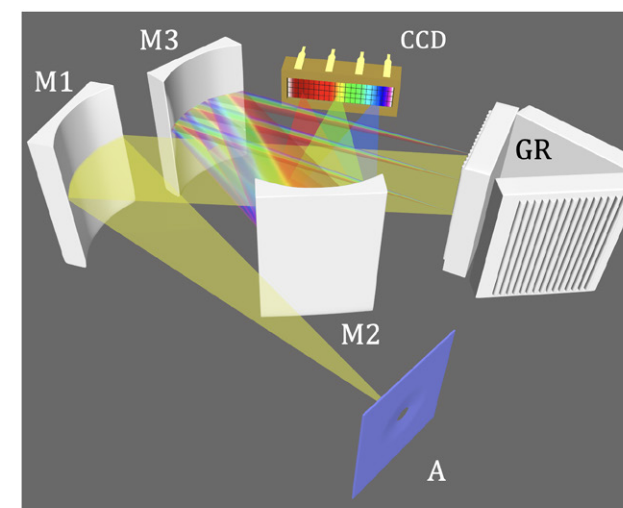


(a)                    (b)

Figure 10. Czerny-Turner (a) and triplet (b) spectrographs: A – pinhole aperture, M1 – collimating mirror, M2 – focusing mirror, M3 – parabolic mirror for aberration correction, GR – rotational turret with diffraction gratings.

The monochromator makes one measurement of the light intensity at a particular wavelength at a time. If a multichannel (array) detector is placed in the focal plane, then all the parallel rays of different wavelengths can be registered simultaneously, and the instrument works as a spectrograph. The spectrograph measures the light intensities at every wavelength and records the entire spectrum in a single snapshot.

The Czerny–Turner design offers flexible and easily configurable setups to fit specific instrument and application requirements. However, the primary issue for a classical Czerny–Turner spectrograph with collecting and focusing mirrors placed symmetrically relative to the grating is astigmatism which results in the spectral resolution varying across the spectrum and depending on the excitation wavelength.

The triplet mirrors spectrograph used in DXR Raman instruments and shown in Figure 10(b) employs an additional focusing parabolic mirror to minimize aberrations. The focusing optics with two mirrors also make the spectral resolution less dependent on the excitation wavelength, resulting in a configuration superior to the Czerny-Turner spectrograph with a single focusing mirror.

There are two important merit figures that allow the evaluation and comparison of the spectrometers' performance: optical throughput and spectral resolution. The presence of an entrance aperture, which restricts the light flux passing through the spectrograph, results in a well-known trade-off between the spectral resolution and optical throughput of the dispersive spectrograph.

## What is the resolving power of diffraction grating?

The most important component of a dispersive spectrograph is the diffraction grating that provides angular dispersion of analyzed light, i.e., spatially separates its constituent wavelengths.

A typical diffraction grating consists of a substrate made of an optical material, with a large number of fine, equidistant, parallel lines (grooves) created on its surface. In a reflective grating, the grooves are created on a reflective surface of the usually metal-coated glass so that light reflects only between the grooves.

The number of grooves per unit length (grove density), usually given in gr/mm, is called the grating constant. The gratings used for applications in the visible spectral range typically have from 600 to 2400 gr/mm. For longer wavelengths, the grating constant should be about 300 gr/mm or less.

The grating constant affects both the wavelength region in which the grating operates and the dispersion properties of the grating. The higher grating constant results in higher resolving power and greater dispersion of the grating. The resolving power $R$ of the grating is defined in terms of wavelengths $\lambda$ and the spectral resolution $\delta\lambda$, the minimal difference between the wavelengths that can be resolved. The resolving power $R$ is a dimensionless number. It can be theoretically shown that $R$ is a product of the order of diffraction $k$ in which the grating is used (typically, $k =1$), and the number of grooves $N$ illuminated on its surface by the incident light:

$$R = \frac{\lambda}{\delta\lambda} = kN.$$

Thus, in order to increase the resolving power of the grating, it is necessary to increase $N$. Accordingly, for the grating of a given width, the grating constant needs to be increased. It is important to note that the collimating mirror in the spectrometer should be aligned to illuminate the grating's full width to provide the theoretically achievable resolving power.

## How does blazed grating increase its diffraction efficiency?

The diffraction grating efficiency can be maximized for a particular wavelength such that most of the light power is concentrated into the first diffraction order $k =1$ for that wavelength and reduced for all other wavelengths. The efficiency optimization can be achieved by appropriate groove shaping, i.e., by making a sawtooth groove profile to form a step structure.

The steps are sloped with respect to the grating surface at the so-called blaze angle, which determines the direction in which the maximum efficiency is reached. Therefore, the grating appears to "blaze" when viewed from that direction. The purpose of the slope of the steps is that the blaze angle θB can be chosen in such a way that the light rays diffracted by the grating, and the rays reflected from the facets of the steps are both deflected in the same direction. Consequently, the angle of diffraction coincides with the angle of specular reflection that significantly increases the diffraction efficiency at a designated wavelength. The wavelength for which the blazed grating is most efficient is therefore specified as the blaze wavelength. As a result, the efficiency can reach over 80% for the specified wavelength. Figure 11 shows the reflective blazing grating principles and typical efficiency curves vs. wavelength for ruled and holographic blazed gratings.
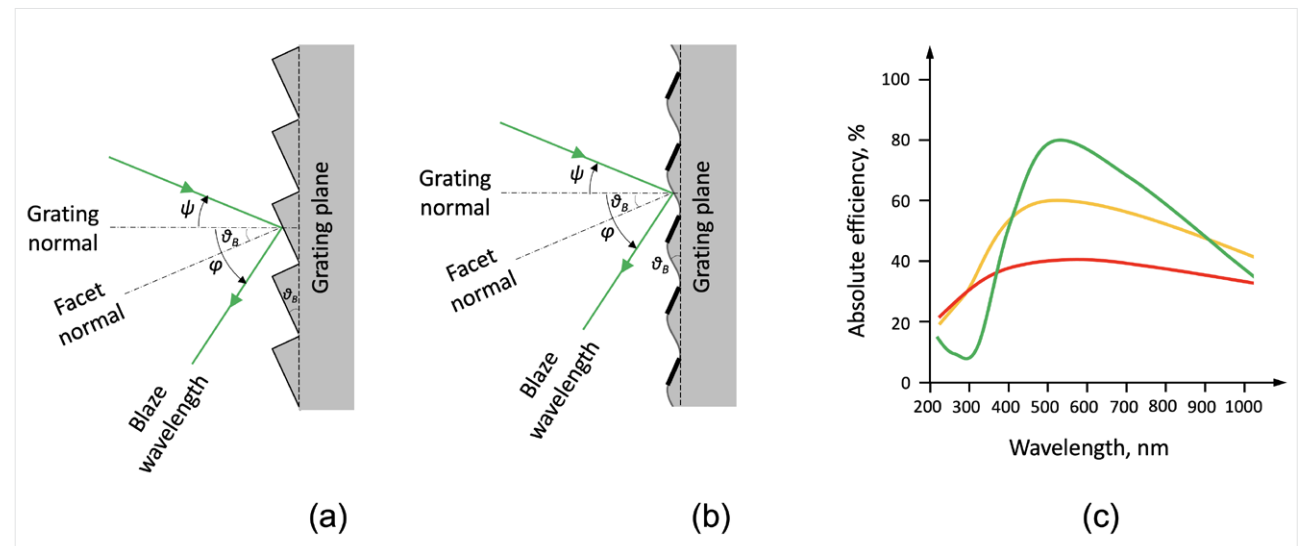


Figure 11. Simplified cross-sections of blazed ruled (a) and holographic (b) diffraction gratings and the typical efficiency curves (c) for ruled blazed at 500 nm (green), holographic blazed at 500 nm (orange) and ruled non-blazed (red) gratings. *(The figure is reproduced by permission from Alexander Rzhevskii, Modern Raman Microscopy: Technique and Practice, Cambridge Scholars Publishing, 2021, 392.)*

The corresponding blazed gratings accompany all the lasers in DXR Raman instruments to increase the optical throughput and sensitivity of the spectrometers.

### How do detector options impact Raman spectra?

The focusing mirror ultimately collects the light diffracted by the grating onto a detector mounted in the focal plane of the spectrograph. A charge-coupled device (CCD) is now one of the most commonly used detectors in Raman spectroscopy. The CCD's major advantage is its high sensitivity to light, which makes it very suitable for detecting inherently weak Raman scattering, and a multichannel principle of operation, which allows the full Raman spectrum to be obtained by the simultaneous measurement of its spectral components. By the full Raman spectrum, we mean the spectrum in the range of wavenumbers corresponding to the fundamental vibrations of the main chemical groups.

A CCD detector consists of a large number of photosensitive elements arranged in a two-dimensional array on the silicon substrate. The discrete elements of the array are called pixels, which is a word that is derived from "PICture ELement". The pixels are defined in the silicon matrix by a grid of current-conducting polysilicon pads called gates. Electrical electrodes are connected to the gates. The entire structure is composed of gates, metal electrodes, an insulating silicon oxide layer and a silicon semiconductor substrate. This structure is known as a metal-oxide-semiconductor (MOS) capacitor, with a photoactive region, also known as the depletion region, to convert photons to electron charge. Shorter wavelengths of light are absorbed close to the surface, while longer wavelengths travel deeper before being absorbed. If the wavelengths of light are long enough (>1050 nm) they do not interact with the depletion region and do not produce a signal.

This is why silicon CCD sensors are not useful detectors for Raman spectroscopy using long wavelength NIR lasers. The conversion rate of incident photons to electron charge is known as quantum efficiency (QE). The higher the QE, the stronger the signal produced by a given number of photons. If noise is assumed to be constant, detectors with higher QE will produce Raman spectra with higher signal-to-noise ($S/N$) values.

The pixels are arranged in rows and columns. The matrices of CCD detectors for Raman spectrographs have a rectangular shape and typically comprise 1024, 2048 or 4086 vertical columns and from 128 to 512 horizontal rows with a pixel size ranging from 13.5 μm to 26 μm.

In a typical dispersive Raman spectrograph, constituent wavelength components of analyzed light are projected onto the CCD array's long axis. Thus, the longer horizontal direction along the rows is ascribed to the dispersion or spectral axis, and the vertical direction along the columns - to the spatial axis, as shown in Figure 12(a).

The major configurations of the CCD detectors for Raman spectroscopy include front-illuminated (FI) and back-illuminated (BI) ones. The principal cross-sections of these CCDs and their typical QE characteristics are illustrated in Figures 12(b,c) and (d), respectively.
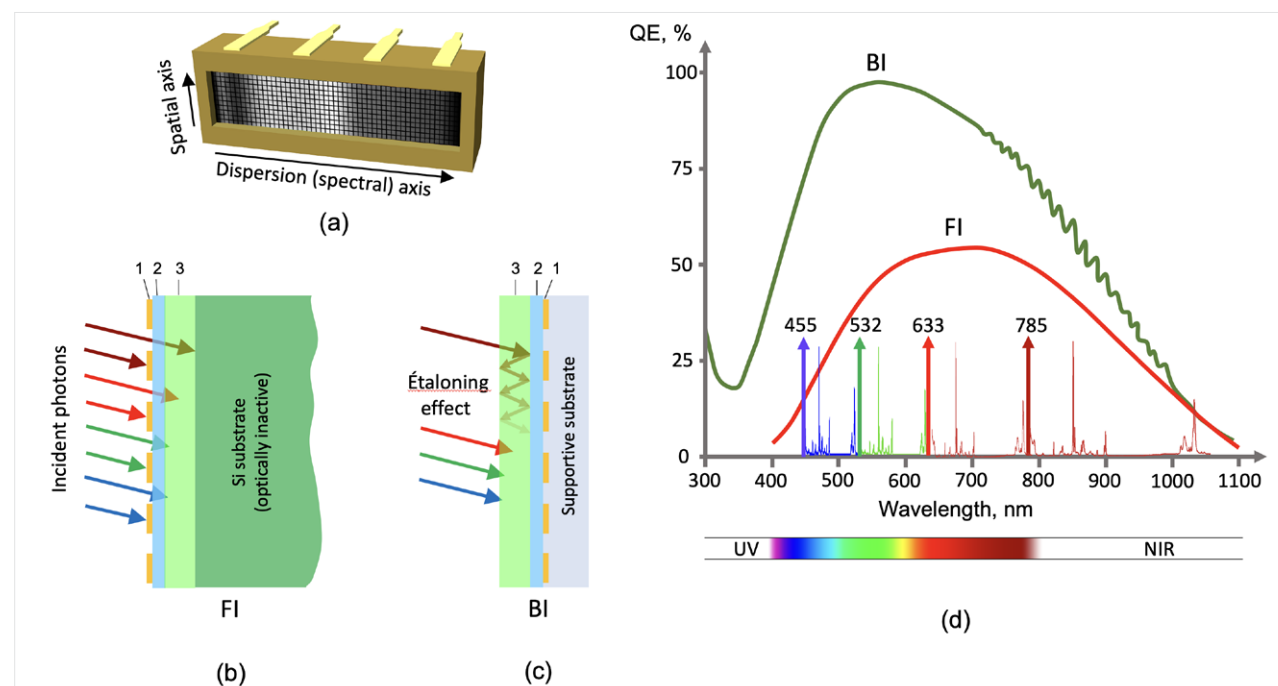


Figure 12. Two-dimensional matrix of CCD detector (a) and simplified cross-sections of front-illuminated (b) and back-illuminated (c) CCD detectors: 1 - gates and electrodes, 2 –insulating layer made of $SiO_2$, 3 - photosensitive region. The incident photons of different wavelengths and their depths of penetration are indicated by the corresponding colors' arrows. The étaloning effect in BI CCD created by deep penetration of long light wavelengths (dark red) through the photosensitive region is shown as multiple reflections from the boundaries of the region. Typical QE characteristics of BI and FI CCD detectors (d): To illustrate how the variation of QE curves with wavelength would modulate the intensities of Raman bands, the spectra of polystyrene in the range of approximately 50–3300 cm$^{-1}$ for the Stokes region are shown for the typical excitation wavelengths of 455, 532, 633 and 785 nm.

The differences between FI and BI CCD sensors arise from how the incident photons get to the photoactive region of the sensor.

In a FI CCD, as shown in Figure 12(b), light photons impinge on the sensor's front surface, which, as mentioned above, is overlaid with a grid of metalized electrodes and polysilicon gates. In this design, the electrodes and gates reflect or absorb some of the photons and thus limit the number of photons that actually reach the photosensitive region. Since fewer photons get to the photosensitive region, this typically limits the QE to around 50–60%.

Alternately, the photons can impinge upon the back side of the sensor (hence, back-illuminated CCD). Since the back of the CCD matrix has no electrodes on it, the surface is clear of any obstacles for the photons to enter the photosensitive region. However, in order to make this work effectively, it is necessary to remove, mechanically or via chemical etching, some of the bulk silicon substrate to provide access to the photoactive region. This is why these types of CCD sensors are also known as back-thinned devices. BI CCDs can attain QEs up to 95%.

The higher QE of BI CCDs would appear to provide a clear advantage. However, there is a drawback. In contrast to the shorter light wavelengths, which are absorbed close to the silicon surface, the longer wavelengths penetrate much deeper into the silicon before being absorbed. This deeper penetration can result in longer wavelengths of light passing all the way through the thinned region and causing constructive and destructive interference by multiple internal reflections at the boundaries of the photosensitive region. This effect is analogous to one in a Fabry-Pérot étalon consisting of a thin, transparent optical medium with two flat, highly parallel and reflective surfaces. Thus, the reflected light creates the étaloning effect, generating an interference fringe pattern. Respectively, the light intensity modulation in the fringes produces the corresponding charge modulation in the photosensitive region. This effect can lead to interference fringes superimposed on a normal Raman spectrum, particularly noticeable in the red and NIR regions. Thus, if a Raman instrument is equipped with BI CCD, then the use of excitation wavelengths of 785 nm and longer is not recommended.

DXR Raman spectrometers can be configured with either FI or BI CCD.

### What does the optical throughput of a spectrograph depend on?

The ratio of the light flux passing through the entrance aperture of the spectrograph to the corresponding flux incident on the detector is called the optical throughput of the spectrograph. The practical optical throughput is determined by the losses of light energy during absorption, reflection and scattering by the optical elements of the spectrograph.

Optical materials used in Raman spectrographs in the wavelength range for which they are intended usually have low absorption coefficients so that the absorption losses, for example, in lenses, do not exceed a few %. Reflection losses are mainly associated with the reflection from the surface of optical mirrors used in spectrographs.

When calculating the total transmission of a dispersive spectrometer, it is necessary to consider all its optical components' efficiency. In the dispersive spectrometers, the total number of surfaces on which reflection or transmission occurs often reaches 14. If we consider the loss on one surface to be 5% on average, then the total transmission will be

$$\tau = (1 - 0.05)^{14} \approx 0.5 \,.$$

The optical throughput of a spectrometer has a direct impact on the sensitivity of the Raman instrument and the amount of time needed to acquire Raman spectra with an adequate $S/N$ ratio. When evaluating the final optical throughput of a Raman spectrometer, it is essential to take into account the efficiency of the CCD detector that was discussed above, as well as the quality of all the spectrograph's components.

## What does the spectral resolution of the spectrograph depend on, and what is the resolution practically required?

The spectral resolution characterizes the ability of an instrument to separate two closely spaced spectral lines. The practical spectral resolution of the dispersive spectrometer is determined by the instrumental function (profile). The narrower the instrumental function, the higher the spectral resolution that can be achieved. The instrumental function depends on the following major parameters:

- the resolving power of the grating: the higher the groove density, the higher the spectral resolution;

- the focal length of the spectrometer: the longer the focal length, the higher the spectral resolution;

- the width of the entrance aperture of the spectrometer: the narrower the aperture, the higher the spectral resolution;

- the pixel size of the CCD detector: the smaller the pixels, the higher the spectral resolution.

The vibrational spectral lines of materials in a condensed phase (liquids and solids) are broadened significantly due to different mechanisms of interactions between the neighboring chemical groups and molecules and their strength (for example, the Van der Waals mechanism or hydrogen bonding). As a result, the typical vibrational spectra of substances in a condensed state consist of individual spectral lines or closely spaced overlapped lines that form spectral bands with bandwidths ranging from several to a few hundred $cm^{-1}$. All the broadening mechanisms form the so-called intrinsic line shape. These mechanisms are divided into homogeneous and inhomogeneous ones and are fairly well described by the Lorentzian and Gaussian functions, respectively.

When both broadening mechanisms are presented simultaneously, which often occurs, the line shape can be given by a convolution of the Lorentzian and Gaussian functions resulting in a Voigt profile.

In general, spectrographs introduce distortion into the intrinsic spectral profiles. If the width of the intrinsic spectral line significantly exceeds that of the instrumental function, then the shape and width of the line recorded by the spectrometer practically coincide with the parameters of the intrinsic line. If the width of the instrument function constitutes no more than ¼ of that of the intrinsic spectral line, then the broadening of the experimentally registered line does not exceed 5%. A spectrograph with a practical resolution of about 4 $cm^{-1}$ is capable of registering an intrinsic linewidth of at least 20 $cm^{-1}$ without any noticeable distortion.

Since the half-widths of the bands in the spectra of solids rarely appear to be narrower than 10 $cm^{-1}$ and, in the spectra of liquids, mostly exceeding 20 $cm^{-1}$, spectrographs that provide spectral resolution in the range of 2–5 $cm^{-1}$ are generally well suited for analyzing samples in a condensed phase. As a rule, compact Raman spectrometers equipped with spectrographs having a focal length between 0.2 m and 0.3 m contain fewer reflective and refractive optical components, increasing their optical throughput. The choice of high spectral resolution is justified for specialized applications or the analysis of gas samples, which is a rather rare task for Raman spectroscopy.

## What is the difference between the spectral and digital resolution of a spectrograph?

Spectrograph manufacturers often prefer to specify the resolution in $cm^{-1}$ per pixel of the CCD detector. This parameter is termed the digital or pixel resolution and usually corresponds to the point spacing in the digitized spectrogram. The digital resolution is related to the Nyquist-Shannon sampling theorem that states that the sampling frequency should be greater than twice the highest frequency in the spectrum. The highest frequency that the spectrograph can detect is determined by its spectral resolution. Consequently, at least two CCD pixels must fall within the spectral resolution value. Otherwise, the size of the pixels will limit the resolution of the spectrograph. Therefore, the digital resolution is two times higher than the spectral resolution.
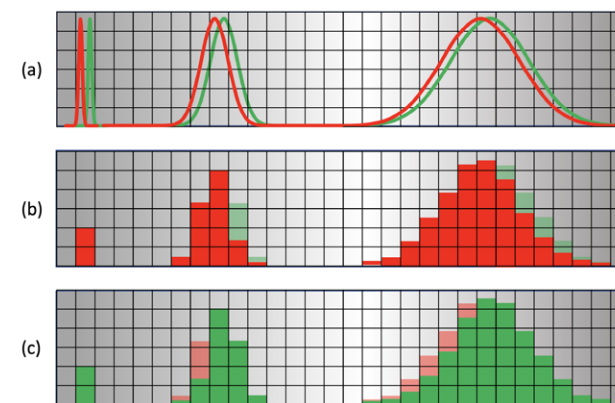


Figure 13. Two closely spaced spectral lines (red and green) projected onto the detector array in analog form (a) and converted to digital form (b and c). The position of the maxima of the lines differs by less than one pixel. The pixel filling histograms shown in (b) and (c) for the red and green lines, correspondingly, demonstrate the coincidence of the histograms for the lines fitting a single vertical pixel column (left) and their mismatch as the lines become broader (middle and right). *(The figure is reproduced by permission from Alexander Rzhevskii, Modern Raman Microscopy: Technique and Practice, Cambridge Scholars Publishing, 2021, 392.)*

Figure 13 illustrates how two closely spaced spectral lines are projected onto the detector array in analog form (a) and conversed to digital form (b–c). The position of the maxima of the lines differs within one pixel. Suppose both the lines are so narrow that they fit entirely in one vertical column of pixels. In that case, such lines cannot be resolved because, regardless of the exact position of the line's maximum within the pixel, the total charge is only accumulated and read out from this column of pixels. If the full width at half-maximum (FWHM) of these lines spans two pixels, as required by the Nyquist-Shannon theorem, these spectral lines are resolved. Indeed, the digital projections of these lines on the detector, as shown by pixel-filling histograms in the columns, do not coincide. When the spectral lines get broader so that their FWHMs occupy several pixels, their maxima's position can nevertheless be determined with adequate accuracy, as long as the corresponding histograms do not completely coincide with each other. Thus, in contrast to the often-repeated misleading statement, determining an accurate position of the band and its shift in the wavenumbers scale does not require spectral resolution equal to or better than the value of the assumed shift. The position of a spectral band can be found quite accurately by calculating the so-called center of gravity of the band or from a curve-fitting procedure.

DXR Raman spectrographs offer a practical spectral resolution of better than 5 cm$^{-1}$ (2 cm$^{-1}$/pixel) for the full Raman spectrum and 2 cm$^{-1}$ (1 cm$^{-1}$/pixel) for the half-spectral range. This resolution is sufficient for the qualitative and quantitative spectral analyses of the majority of liquid and solid materials.

## What is the benefit of the spectrograph with fixed-position diffraction grating?

Several diffraction gratings, often with different groove density and, consequently, resolving power, is usually mounted on a rotational turret. A triple-grating turret is a standard option available in many Raman spectrographs. The drive mechanism rotates the turret to select a grating and turns the selected grating around its pivot axis to set an operational wavelength. As an example, Figures 14(a) and (b) illustrate the process of acquisition of a Raman spectrum of polystyrene by sequentially projecting two halves of the spectrum onto CCD by turning a diffraction grating GR1. When the turret rotates and replaces the grating GR1 by GR2 with half the dispersion, the full spectrum is projected onto the CCD and acquired in one pass, but with half the spectral resolution (c).

This practice of turning the grating, acquiring the spectrum in multiple spectral regions and stitching the regions together using spectroscopic software is often applied in Raman instruments. Despite the significant advantages of multi-grating turrets, moving the gratings has a few shortcomings. First, it takes time to move between grating positions and, if a broad spectral coverage is required, collecting multiple regions may be too time-consuming for fast spectral imaging or reaction monitoring applications. Second, as the different regions of the spectrum are acquired at different times, continuous reaction kinetics measurements appear to be problematic. Third, the grating mechanical drive inevitably yields errors in the accuracy and repeatability of the grating position when turning the grating that, correspondingly, introduces inaccuracies in optical performance and the Raman spectra.
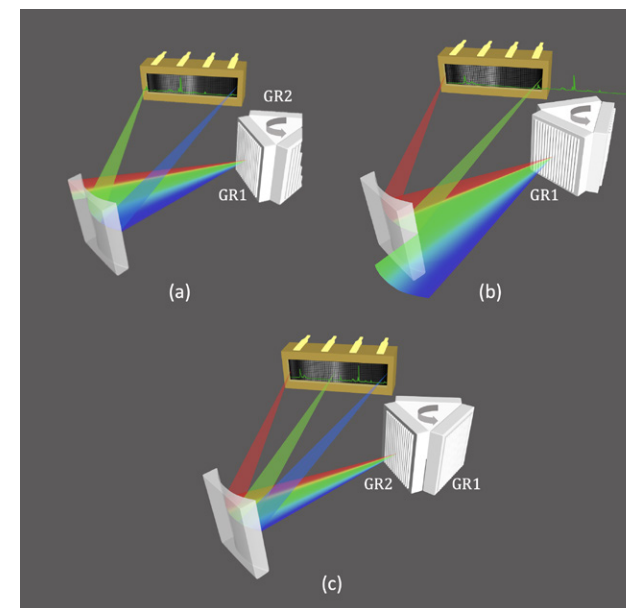


Figure 14. Acquisition of a Raman spectrum using diffraction gratings on a rotational turret. In (a) and (b), two halves of a spectrum are sequentially projected onto CCD and acquired using the diffracting grating GR1. In (c), the full spectrum is projected and acquired using GR2 grating with half the dispersion and, respectively, half the spectral resolution. The Raman spectrum of polystyrene is shown as an example. *(The figure is reproduced by permission from Alexander Rzhevskii, Modern Raman Microscopy: Technique and Practice, Cambridge Scholars Publishing, 2021, 392.)*

These shortcomings are addressed by using a fixed position grating that directs the full spectral range of most interest in Raman spectroscopy (for example, from 50 to 3500 cm$^{-1}$) to the array detector while maintaining adequate spectral resolution.

All DXR Raman spectrographs contain no rotating turret but fixed-position interchangeable blazed-angle gratings.

# Raman Microscopy

## What is Raman microscopy?

In a Raman microscope, a research-grade optical microscope is coupled to a laser excitation source and spectrometer, thereby constituting a scientific instrument capable of obtaining both traditional optical and spectrochemical images with a spatial resolution at the diffraction limit of light (<1 micron). The Raman microscope enables the measurement of chemically and spatially inhomogeneous samples to reveal their chemical composition, morphology, molecular orientation, conformation, polymorphism, crystallinity, material deformation, local temperature, etc. A 3D spectrochemical representation of the sample can be constructed by acquiring 2D area images at different depths in a confocal mode by sequentially shifting the laser focus inside a transparent or translucent sample. This method of 3D spectrochemical imaging preserves the sample integrity and avoids possible artifacts that may result from physically cutting or sectioning the sample. No other microscopic technique offers such a combination of spatial resolution and "information-reach" spectral content within a workable acquisition time.

The principle diagram and a description of a dispersive Raman microscope are given above (see Figure 7).

## What is the role of a confocal aperture (pinhole)?

The paths of the light rays in the Raman microscope and the function of a confocal aperture are illustrated in Figure 15. The light rays from the laser and the rays collected by the microscope objective from the focused laser beam are denoted in green, while the rays entering the spectrometer are yellow. As the circular aperture (pinhole) is placed in the image plane of the microscope, the pinhole is confocal with the focal point. The principal role of the confocal pinhole is to filter the light rays collected by the microscope objective spatially and to pass the selected rays through the pinhole to the spectrograph.
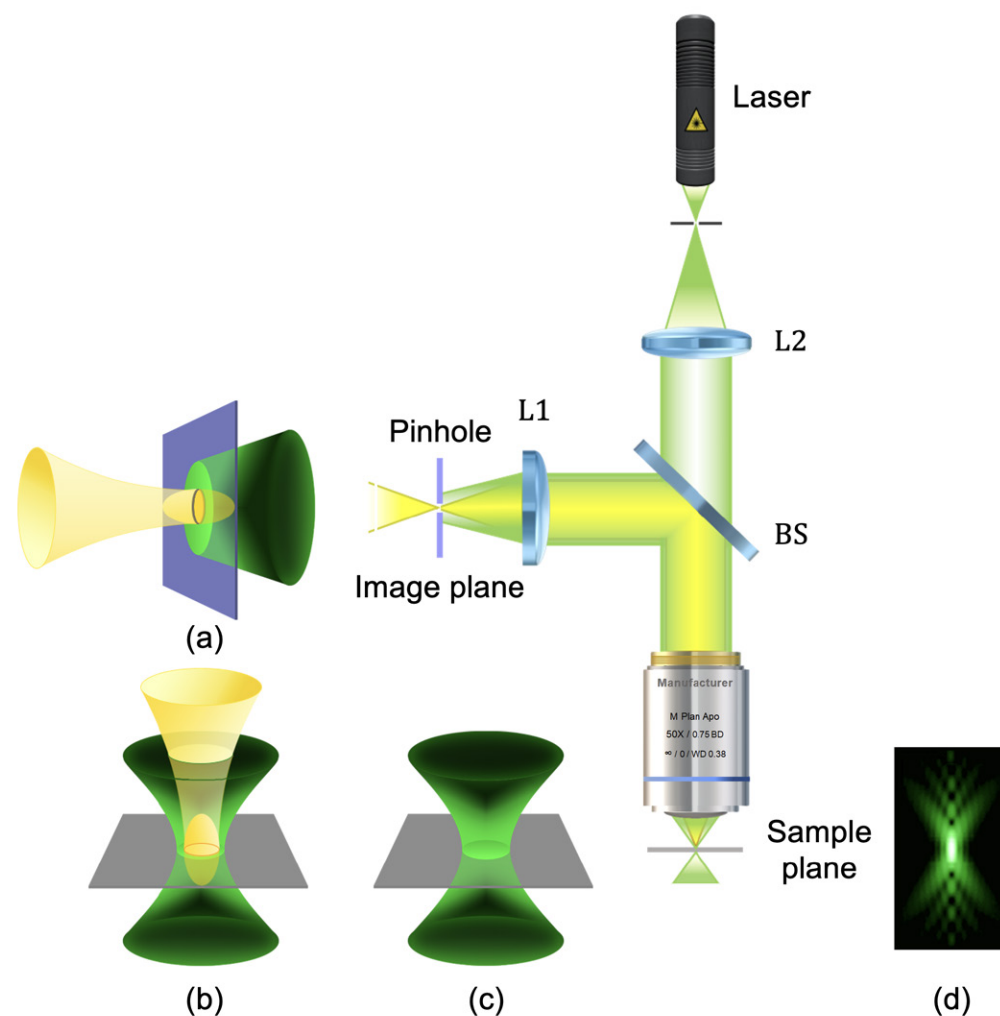


Figure 15. The role of a pinhole in a confocal Raman microscope. The paths of light rays emitted by the laser and collected by microscope objective (green) and the rays "observed" by the spectrograph through a confocal pinhole (yellow) are shown in the center, where BS is a beamsplitter, and L1 and L2 denote the focusing lens and the laser beam expander lens system, respectively. *(The figure is reproduced by permission from Alexander Rzhevskii, Modern Raman Microscopy: Technique and Practice, Cambridge Scholars Publishing, 2021, 392.)*

The laser beam focused by the objective converges in the form of a cone in the focal plane and then diverges in the same way. The volume illuminated by the focused laser beam can be depicted as a green hourglass shape, as shown in Figure 15(c). The objective collects the light scattered from this hourglass shape; it is then magnified and projected onto the image plane. The light rays emanating from the converging and diverging cones above and below the focal plane are combined to form a converging green cone in the image plane. When a pinhole is placed in the image plane, it blocks all the rays emanating from the out-of-focus regions and allows only the rays from a small volume around the focal point to pass through. The small volume can be represented by the prolate spheroid "spread" out along the optical axis. This prolate spheroid is highlighted in yellow in Figure 15(a). Since the image and sample plane are conjugated, the spheroid can then be projected back onto the sample plane to visualize the small volume element from which the spectrograph measures the scattered light. Thus, the confocal aperture ensures that only the light emanating from the spatially discriminated volume depicted by the yellow spheroid inside the green hourglass shape in Figure 15(b) passes from the laser focus to the spectrometer.

The effect of the attenuation of the out-of-focus regions represents spatial filtering and can be described in terms of the point spread function (PSF). The volume element measured in the confocal mode is determined by the so-called effective optical PSF. It is a product of the hourglass shape illuminated by the laser and the volume of the spheroid "observed" by the spectrograph through the pinhole. An effective PSF constitutes one of the essential properties of the confocal Raman microscope.

In a non-confocal mode, when the aperture is a slit, the Raman spectrum measured by the spectrometer represents Raman signals emanating from the entire hourglass shape. Suppose this shape comprises chemically different and spatially separated microdomains. In that case, the recorded Raman spectrum is the superposition of Raman spectra of all these microdomains, and they will not be discriminated spatially. A significant improvement in the spatial discrimination is obtained in both the lateral (perpendicular to the optical axis of the objective, i.e., in the horizontal XY plane) and axial (along the optical axis, i.e., in the vertical Z-axis) directions in the confocal mode of operation.

By varying the diameter of the confocal aperture, operators of Raman microscopes can select the volume element to measure at a given objective magnification and optimize the intensity in the Raman spectra of the materials under study. A confocal aperture with the ability to continuously vary its size is often called a confocal diaphragm. The confocal diaphragm is advantageous for precise confocal Raman microscopy.

### How important are optical alignment and calibration?

Optical alignment and calibration are two important practices that must be routinely executed for the optimal performance of any high-end Raman microscope.

In the course of time, all Raman microscopes are subject to alignment and calibration drifts. These drifts may be caused by laboratory temperature fluctuations, external disturbances of the instrument, normal wear of system components occurring during regular operation, and many other factors.

A proper confocal configuration of a Raman microscope means the spheroid is well centered within the hourglass shape, as illustrated above. The process of bringing the laser focus and the volume element "observed" by the spectrometer into a perfect coincidence is known as alignment. The regular alignment compensates for variations caused by the inevitable drift over time. A correctly aligned confocal Raman microscope provides the best spatial discrimination at a high intensity of the Raman spectrum.

Calibration is another procedure that ensures the accuracy of the experimentally measured Raman spectrum with the correct Raman shift and spectral intensity. Unlike FT-IR instruments with a built-in "internal standard," a laser that monitors the optical path difference in the interferometer and provides accurate wavenumber measurements, dispersive Raman instruments must use samples or standards that have spectral peaks with known Raman shifts for calibration. Raman spectra obtained with different lasers may have significant variations in the relative peak intensities, mainly due to wavelength-dependent differences in the quantum efficiency of the CCD. The intensity difference can be adjusted using the so-called white-light correction technique. The white-light correction is an intensity normalization procedure that may utilize a broadband white-light radiation standard applicable to multiple excitation wavelengths. This procedure establishes a scaling factor to correct the intensities depending on the wavelength along the Raman shift axis.

Manually performed alignment and calibration routines usually require a certain level of qualification for the maintenance personnel and additional materials and sources; it also often increases the downtime of the instrument during the operation.



Figure 16. The alignment and calibration tool to be placed on the microscope stage (a), and the bright pinhole of the tool in the optical focus centered on the microscope eyepiece crosshair (b).

In DXR Raman microscopes, alignment and calibration are highly automated procedures, simplifying their implementation and eliminating user error or subjectivity. These procedures are performed in a software-controllable manner using a dedicated matchbox-sized tool placed on the microscope stage. The user handles this tool as a sample and focuses on a small pinhole in the center of the box, as shown in Figure 16.

## What does spatial resolution in confocal Raman microscopy depend on?

When a microscope objective focuses the laser beam, the illuminated volume can be determined by the space enclosed by an hourglass shape shown above in Figure 15(c). This volume is characterized by its "waist" or the diameter of the laser spot in the XY focal plane approximated by the Airy disk:

$$d_{xy} = \frac{1.22\,\lambda}{NA},$$

(11)

where $\lambda$ is a laser excitation wavelength, and $NA$ is the numerical aperture of the microscope objective.

Hence, the higher $NA$, the smaller the spot that can be produced by the objective passing the light of a given wavelength. The spot size is directly related to the lateral spatial resolution in the Raman microscope since the incident light is focused in, and the scattered light is collected from this spot. The lateral spatial resolution is generally defined as the shortest distance between two objects in the focal plane, which can be resolved. The spatial resolution is evidently better and is termed "higher" when the laser spot is smaller. A sub-micron lateral spatial resolution can be achieved for visible excitation wavelengths using objectives with a higher $NA$. The relationship between the laser spot diameter and $NA$ is illustrated in Figure 17.

Consider an example of the diffraction-limited illumination of the sample with a 532 nm excitation light using an objective with $NA = 0.9$ and 100× magnification (100×/0.9). According to equation (11), the diameter of the focused laser spot will be 0.72 µm at the sample plane. The spot will be projected onto the image plane with magnification by a factor of 100.
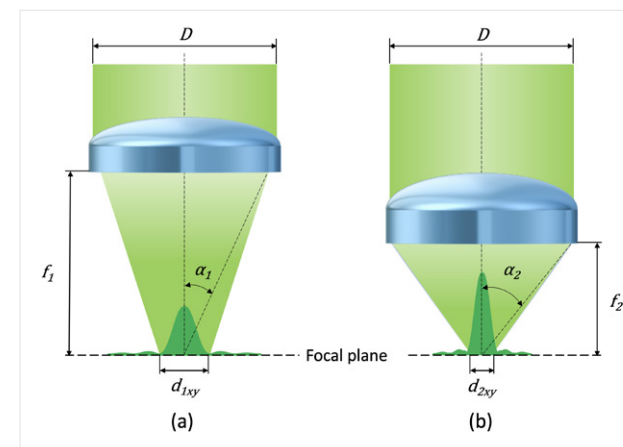


Figure 17. Diffraction-limited focused laser spot produced by objective lenses with low (a) and high (b) $NA$: $D$ is the diameter of the laser beam that illuminates the lens; $f_1$ and $f_2$ – focal lengths; $\alpha_1$ and $\alpha_2$ – the half-angles of the cone of light that exits the lens; $d_{1xy}$ and $d_{2xy}$ – diameters of the laser spots for low and high $NA$, respectively. The diffraction pattern of focused light in the plane perpendicular to the focal plane with the central Airy disk and a few sidelobes is shown in dark green. *(The figure is reproduced by permission from Alexander Rzhevskii, Modern Raman Microscopy: Technique and Practice, Cambridge Scholars Publishing, 2021, 392.)*

Assuming that the image plane coincides with the spectrograph entrance, the beam diameter will be 72 µm at the spectrograph entrance. If a confocal pinhole with a diameter of 50 µm is set at the entrance of the spectrograph, then only part of the light from the 72 µm beam spot can pass through the pinhole and reach out to the detector. Thus, a pinhole size that is less than the diameter of the laser spot projected onto the image plane will improve the lateral spatial discrimination by a factor of about 1.4. However, the improvement in the lateral spatial discrimination is accompanied by a significant loss in the intensity of the Raman signal, and factor 1.4 is considered to be an optimally achievable improvement in practice.

The depth of the region illuminated by a laser in the axial Z direction can be estimated using the following equation:

$$d_z = \frac{2.53\,\lambda}{NA^2}.$$

(12)

Dividing (12) by (11), the ratio of $d_z$ to $d_{xy}$ is derived as

$$\frac{d_z}{d_{xy}} = \frac{2}{NA}.$$

When the laser beam is focused in air, the depth of focus appears to be more than twice the size of the laser spot since the maximum $NA$ of an objective operating in the air does not exceed 0.95:

$$\frac{d_z}{d_{xy}} > 2.$$

However, the illuminated region in the Z direction from which the Raman spectrum is collected in a condense-phase sample has to include the refractive index of the sample $n$ so that:

$$\frac{d_z}{d_{xy}} > \frac{2n}{NA}.$$

In the confocal arrangement, the height of the sampling volume element, called the confocal depth, can be estimated using a PSF. Practical calculation of an effective PSF is a complicated task that requires taking the details of the optical design of a given confocal Raman microscope, the quality of its optical components, the characteristics of the laser beam and many other factors into account.

Nevertheless, the confocal depth determined by the major axis of the prolate spheroid shown in Figure 15(b) and Figure 18 may be approximated by the following equation:

$$d_{PSF} = \sqrt{\left(\frac{0.88\lambda}{n - \sqrt{n^2 - (NA)^2}}\right)^2 + \left(\frac{\sqrt{2}\,nD_{PH}}{NA}\right)^2},$$

(13)

where DPH represents the diameter of the pinhole projected back onto the sample plane, which, in general, can be calculated in micrometers if one knows the total magnification factor of the microscope with a given objective.

As it follows from equation (13), for the excitation wavelength $\lambda$ and the objective with a given $NA$, the first term under the root is constant, and the confocal depth is influenced exclusively by the pinhole diameter in the second term.

The depth discrimination improves (the confocal depth decreases) as the excitation wavelength shortens and the pinhole diameter reduces. It is logical to assume that making the pinhole as small as possible is the best option for depth discrimination. However, as the pinhole size reduces, the amount of light collected from the sample and reaching the detector also decreases. Because the Raman scattering is intrinsically weak, pinhole apertures with diameters smaller than 25 µm are rarely used and are only practical for materials featuring strong Raman scattering cross-sections $\sigma$.
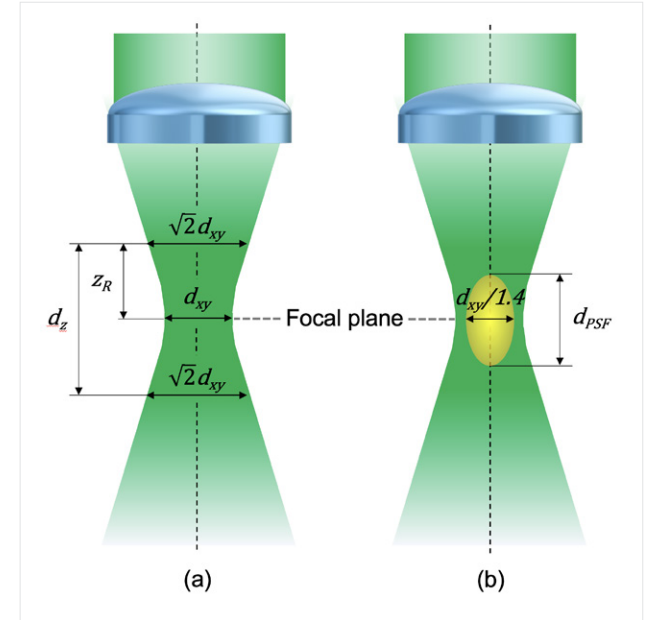


Figure 18. Diameter $d_{xy}$ and depth of focus $d_z$ of the focused laser beam (a) and the confocal depth $d_{psf}$ (b). The height $d_z$ is determined as two $z_r$ (Rayleigh range), the distance between the two planes at each side of the focused spot where the width $d$ of the beam is a factor of $\sqrt{2}$ larger than it is at the focus and, consequently, the area of the beam cross-section is doubled, and the brightness is taken to be equal to one-half of the maximal brightness of the beam at its focus. *(The figure is reproduced by permission from Alexander Rzhevskii, Modern Raman Microscopy: Technique and Practice, Cambridge Scholars Publishing, 2021, 392.)*

Thus, using the confocal pinhole improves both the lateral and axial spatial discrimination and particularly accounts for the ability of the confocal Raman microscope to provide optical sectioning of a sample. In order to achieve higher spatial discrimination, a shorter excitation wavelength, an objective with higher $NA$ and a smaller confocal pinhole should be used.

It needs to be emphasized that, in practice, the confocal aperture does not restrict the sampling volume element to a prolate spheroid with a sharp boundary depicted in Figures 15(b) and 18(b).

The measured Raman intensities may fall off fairly slowly on either side of the focal plane in the axial direction. The relatively slow decay in the *Z*-axis is in marked contrast to the relatively tight confinement in the XY plane. This slow decay means that in certain circumstances, one can detect significant out-of-focus Raman signals a long way above and below the nominal focal plane, which are well outside the calculated confocal depths.

### What is the difference between a Raman map and a Raman image?

Confocal Raman microscopy is widely used to measure and image the chemical and physical properties of samples in one, two and three dimensions.

Raman spectral image acquisition is essentially a two-step process. The first step is mapping, which is the process of measuring Raman spectra at predetermined locations in a sample. The mapping is typically carried out by means of a laser beam focused at a point sequentially scanned across the selected area. The area and the measurement locations are determined by the operator of a Raman microscope and controlled by proper software.

One of the most attractive features of confocal Raman microscopy is the ability to perform a nondestructive analysis of a transparent or translucent sample at different depths. Assuming the confocal Raman microscope is properly aligned, the focused laser beam may be stepped through the sample perpendicular to its surface. At the same time, Raman spectra are recorded in the so-called depth profiling mode. Collecting an area (XY) map in a plane parallel to the sample surface at a distance *Z* below the surface (probing distance), a spectrochemical image deep within the sample can be obtained by analogy with the image produced by optical sectioning microscopy.

This technique is referred to as Raman optical sectioning because it does not require mechanical cutting or sectioning of the sample. Collecting maps successively at different probing distances with typically a regular interval along the vertical *Z*-axis, a 3D representation of the sample may be constructed. In general, the maps may be collected along a line or from an area in both horizontal and vertical planes or a sequence of areas along the vertical axis to render a volume of the sample.

The second step is spectrochemical image generation. The image is constructed by processing the array of spectral data in the corresponding maps in various ways, e.g., as parameters of an individual spectral peak, the ratio of peak intensities, correlation with a reference spectrum or based on more complex chemometric and statistical methods of the analysis commonly used in optical spectroscopy. A meaningful number of Raman images generated from a map is determined by the distinguishable spectral features associated with the different sample constituents or properties.
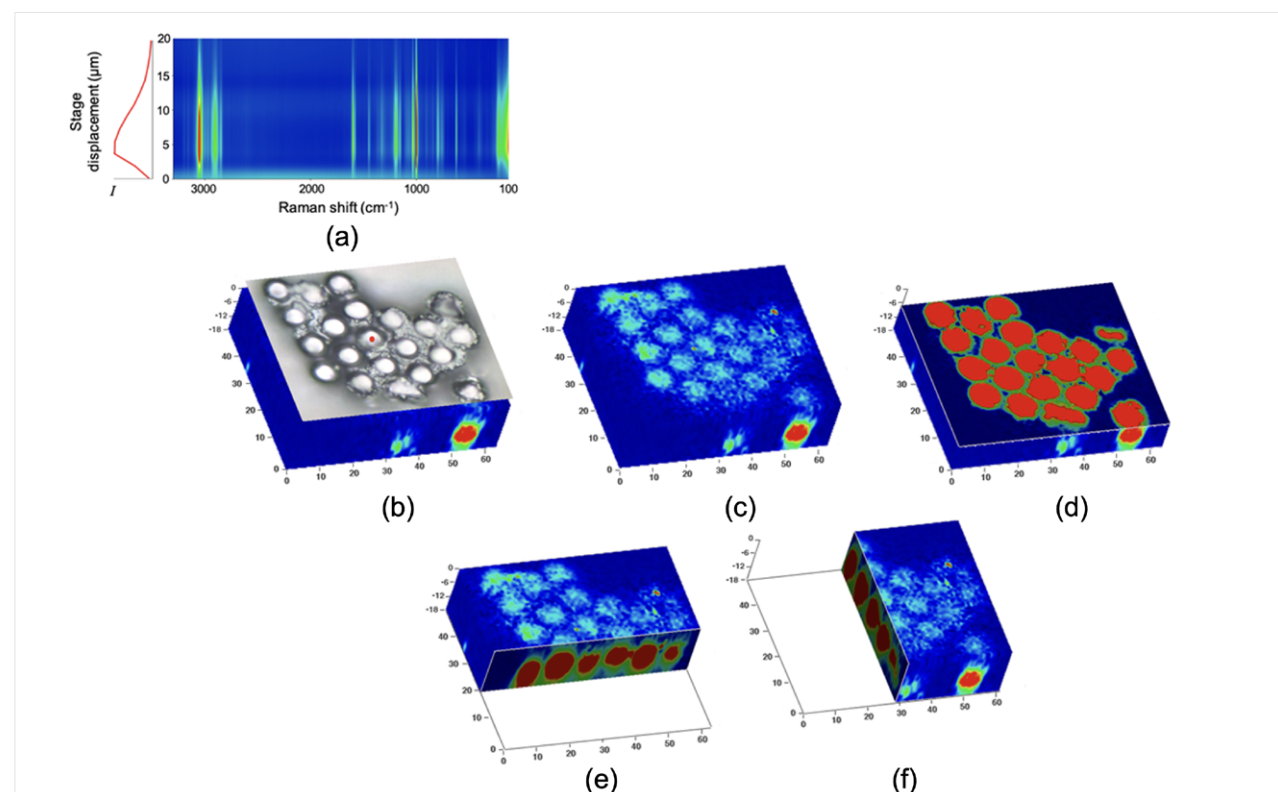


Figure 19. (a) The depth profiles of an individual polystyrene spherical particle from the cluster of the particles with diameters of about 10 μm embedded in a glass matrix measured at the point indicated by the red dot in (b). In the depth profiles, the integrated intensity *I* of the polystyrene band at 1001 cm$^{-1}$ (the left inset) and the intensities of the Raman bands of polystyrene in the spectral range of 100-3200 cm$^{-1}$ (the right inset) are shown as a function of the sample stage displacement in Z-axis. Rendering the Raman spectral image obtained from a cluster: (b) optical image of the sample surface superimposed on the 3D Raman image; (c) the 3D Raman image shown without the optical image; (d) the XY section at a probing distance of 8 μm; (e) an XZ section of the 3D image; (f) a YZ section of the 3D image. The red color shows the highest intensity of the band at 1001 cm$^{-1}$ in the Raman spectrum of polystyrene and, consequently, highlights the polystyrene particles, while the blue color corresponds to the glass matrix.

Theoretically, the maximal number of spectrochemical images that may be generated from a single map is equal to the number of resolved spectral elements. Since humans can easily recognize visual targets based on colors, the processed data outcomes are usually visualized in pseudo-colored Raman images with different color schemes or patterns. In the most commonly used pattern designed around the three primary colors and categorized as warm and cool, the red and blue colors are designated, respectively, to the highest and lowest values of the outcomes.

Thus, depending on the map's geometry, Raman spectrochemical images can be represented by color-coded lines, areas or volume structures in which the colors indicate the spatial distribution of chemical components or sample properties. As an example, Figure 19(b–f) shows a 3D Raman spectral image acquired within a rectangular box of a sample composed of 10 µm polystyrene beads embedded in a glass matrix. The 3D Raman image is generated as the integrated intensity of the spectral band of polystyrene at 1001 cm⁻¹. The depth profile of an individual particle from the cluster is represented in Figure 19(a).

### What is the advantage of oil immersion over a "dry" metallurgical objective?

It should be emphasized that when performing spectral measurements using a metallurgical ("dry") objective (the most common commercial choice) beneath the surface of a sample with a refractive index $n$, the effect of refraction at the air/sample interface shifts the point of focus much deeper into the sample than the sample displacement in the vertical Z direction designates. As a result, the depth scale appears to be falsely compressed, as depicted in Figure 20(a).
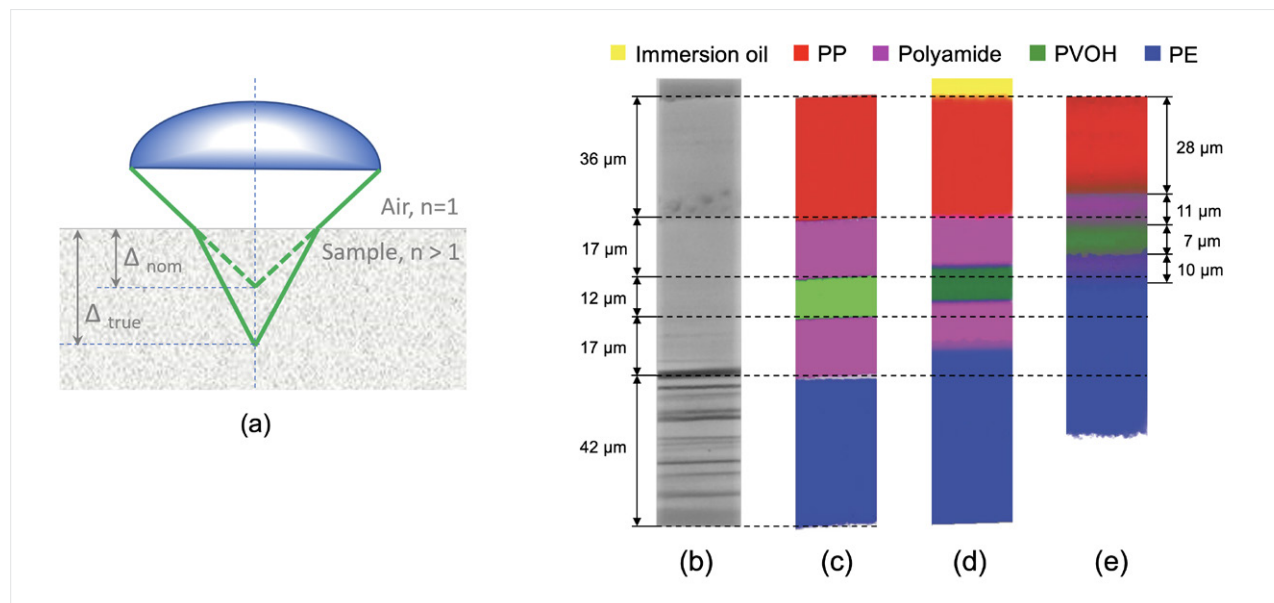


Figure 20. (a) When a metallurgical objective is used to focus the laser beam and make spectral measurements below the sample surface, the point of focus is shifted into the sample by distance $\Delta_{true}$, which is deeper than the sample displacement $\Delta_{nom}$ designates due to the refraction at the interface between the sample (refractive index n > 1) and air (n = 1). Optical and Raman spectral images of a multi-layer polymer film: (b) optical image of a mechanical cross-section cut, (c) Raman image of the cross-section cut, (d) Raman optical section obtained with 100×/1.3 oil immersion objective, (e) Raman optical section obtained with 100×/0.9 metallurgical objective,

Immersion objectives with a fluid that matches the refractive index of the sample may be used to minimize the problem of laser beam refraction at the air/sample interface. Filling the gap between the objective's lens and a sample with an index-matching fluid removes the bending of the light at the surface of the sample caused by refraction. An oil immersion objective can be used for confocal Raman measurements within polymers since the refractive index of oil ($n$ = 1.52) is close to that of many polymer materials.

A common application of Raman confocal depth analysis is the investigation of multi-layer polymer composites. 2D Raman images of a layered polymer composite approximately 124 µm thick and consisting of 5 distinct layers obtained using both a metallurgical objective and an oil immersion objective are shown in Figure 20. The Raman images are generated using a multivariate curve resolution (MCR) algorithm. MCR analysis is a powerful analytical tool because it allows spectrally discriminating sample components without requiring any direct knowledge of the Raman spectral features of the components prior to analysis.

As a reference, Figure 20(c) shows the results of imaging of a physical cross-section of the same polymer composite. When using the metallurgical objective, there is clearly a significant compression of the layers compared to what is observed in both the Raman image obtained from the cross-section and using the oil immersion objective. In contrast, the layer thicknesses determined from the image collected with the oil immersion objective and the image of the cross-section are in close agreement. It is also evident that the layers in the confocal image using the metallurgical objective are less well defined due to a loss of spatial resolution, leading to increased mixing of the spectral features at the interfaces between the layers. This issue also contributes to additional uncertainty in the layer's thickness determination. Using oil instead of air between the objective and the sample restores the spatial discrimination, eliminates the depth scale compression and increases the amount of scattered light collected at the probing depth.

### What is the difference between CCD and EM-CCD detectors?

CCD and electron multiplying (EM-CCD) are the most common choices for detectors in Raman microscopes. The detectors operate on the same basic principles considered above. However, EM-CCD detectors are different from CCD ones in that they employ a multiplication register to amplify charges, as shown in Figure 21. As the charge is being transferred for read out, it passes through a multiplication register. The register consists of a large number of cells where high voltage is applied to impart additional energy to the electrons. When an electron has sufficient energy, impact ionization can occur, and this creates an additional electron-hole pair.
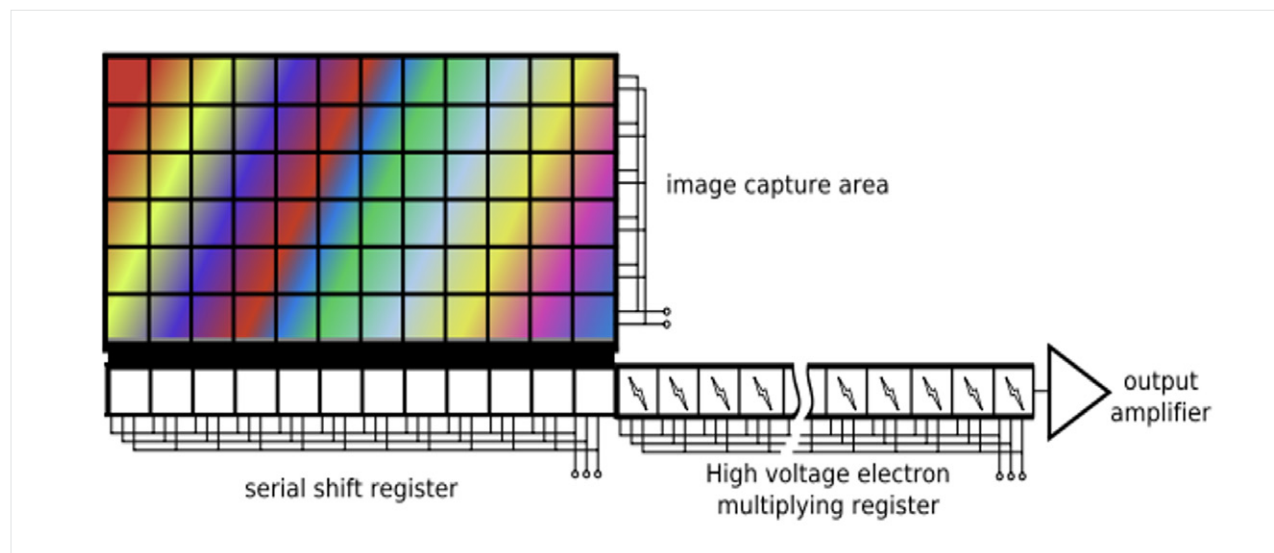


Figure 21. Schematic of EM-CCD detector with the electron multiplying register.

In this way, an additional charge is created, effectively amplifying the signal. The gain is controlled by adjusting the applied voltage, which affects the probability that impact ionizations will occur. The multiplication register amplifies any charge and thus amplifies charges associated with the signal and charges associated with different types of noise. However, since the read noise is not multiplied, it becomes essentially insignificant when using an EM-CCD and thus is not a limiting factor of the $S/N$ of the camera. EM-CCD detectors excel in situations that benefit from faster read-out speeds (short exposures and multiple exposures). Faster read out also reduces dark current noise. Thus, EM-CCD detectors are capable of achieving relatively high $S/N$ when operating at these faster rates.

The advantage of the EM-CCD camera is lost as longer and longer exposure times are used. Longer exposure times might be required because the samples of interest are weak Raman scatter. Longer exposure times result in an increased signal because the camera is exposed to impinging photons for longer. In those situations, the camera is read less often, and the relative effect on read noise is diminished while the noise factor associated with the amplification process remains. It should be noted that an EM-CCD can be operated with the amplification turned off (gain =1) in which case it operates essentially like a standard CCD camera.

## How to select the appropriate step upon mapping?

The design and characteristics of the sample scanning mechanisms and techniques are important as they determine the way and the rate at which the Raman map is collected. Conventional instruments are equipped with mechanical stages driven by stepper motors, while high-speed imaging systems use sampling mechanisms based on the raster scanning principle. The main difference is that the former scans the samples in a discrete point-by-point, also called stop-and-go mode, while the latter allows scanning continuously without stopping, which is a critical factor for fast mapping.

This mode offers the same size of the laser spot at each point and adequate precision of their positioning on the map. However, the motion of the mechanical stages in the intermittent stop-and-go regime results in a longer acquisition time than other mapping techniques.

DXR Raman Microscope is provided with an automated XYZ mechanical stage, while DXRxi Raman Imaging Microscope is equipped with a magnetic linear motor stage and electron-multiplying EM-CCD detector. This stage moves continuously in a zigzag manner while the EM-CCD is read out at certain intervals determined by the sampling step and exposure time. The spectrum accumulates while the stage is moving so that the resultant Raman spectrum is obtained from a linear segment of the sample rather than a discrete point. The area of the segment is determined by the laser spot size multiplied by the sampling step: that is, the distance that the stage passes for a predetermined exposure time.

The speed of the stage movement $v_{stage}$ is usually controlled by software based on the sampling step equal to the linear segment $l_s$ divided by the exposure time $t_{exp}$ defined by the operator:

$$v_{stage} = \frac{l_s}{t_{exp}}.$$

This method allows the map of a relatively large sample area to be acquired with high spatial precision and a fast speed. The measurement of the linear segment results in a better opportunity to detect Raman scattering from a small object.

In Raman microscopy, the smallest object that can be captured and measured is determined by the focused laser spot size and the distance between the points of the mapping grid, usually referred to as the sampling step. There are three principal mapping conditions that set the relationship between the laser spot and the sampling step:

- Par-sampling: the laser spot is equal to the step size;
- Under-sampling: the laser spot is smaller than the step size;
- Over-sampling: the laser spot is larger than the step size.
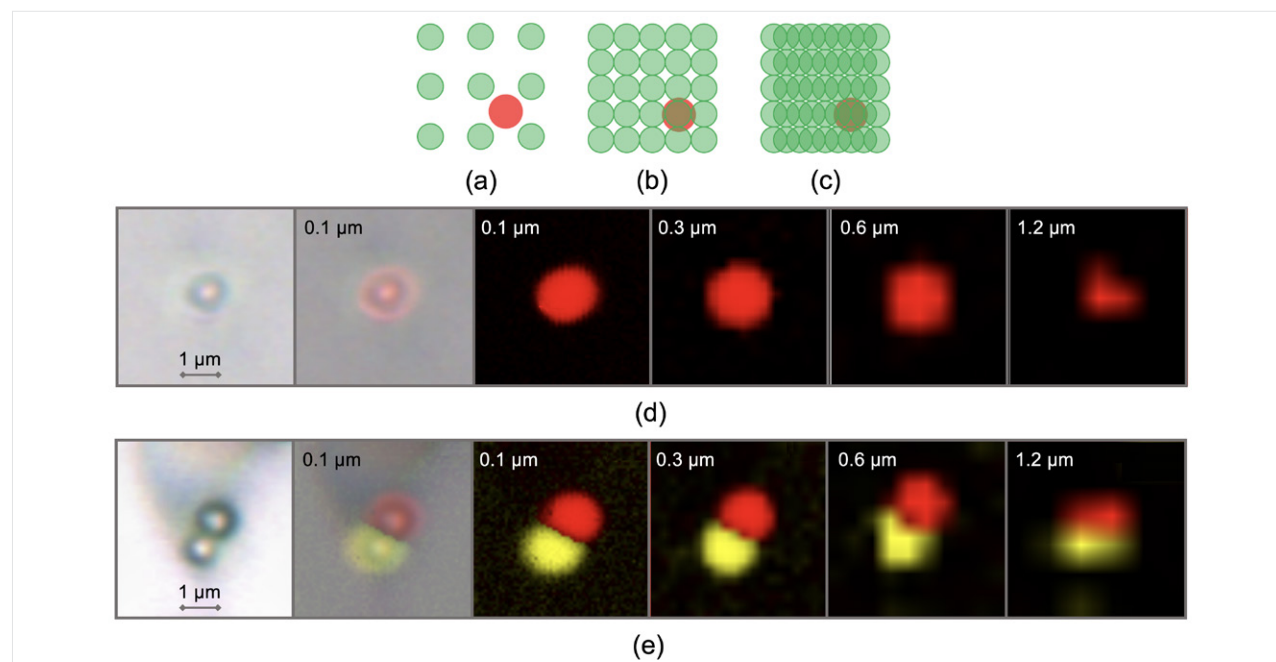


Figure 22. The relationship between the sizes of the sample, laser spot and the sampling step. The green and red circles represent the laser spot and a small sample, respectively, in the schematic of the conditions of under-sampling (a), par-sampling (b) and over-sampling (c). The Raman images of individual polystyrene (PS) bead (d) and the adjacent PS and polymethyl methacrylate (PMMA) beads (e) are constructed from the maps acquired using a 532 nm laser for excitation, 100×/0.9 objective and different sampling steps. The Raman images are generated as spectral components extracted by the MCR method with the red and yellow colour highlighting PS and PMMA, respectively. From left to right: optical images of the beads observed using 100×/0.9 objective, semitransparent Raman images (0.1 μm mapping step) superimposed on the optical images of the beads and Raman images constructed from the map collected at 0.1, 0.3, 0.6 and 1.2 μm steps. *(The figure is reproduced by permission from Alexander Rzhevskii, Modern Raman Microscopy: Technique and Practice, Cambridge Scholars Publishing, 2021, 392.)*

Under-sampling is generally employed when a sample needs to be evaluated, especially at a preliminary phase of the spectroscopic experiment. If there is enough *a priori* knowledge about the sample composition, as well as the distribution of its components and their sizes and shapes, then par-sampling or properly selected under-sampling conditions can be used. Over-sampling can improve the precision and contrast in Raman images, but it requires longer acquisition times and does not improve spatial resolution.

Figure 22 schematically illustrates the relationship between the laser spot and step size in an area map when the laser spot size and dimensions of the object are comparable. Obviously, under-sampling may result in missing the microscopic object (red circle) present in the sample, while par-sampling and over-sampling ensure the object is captured.

The examples of mapping an individual polystyrene (PS) bead and a PS bead adjacent to a polymethyl methacrylate (PMMA) bead using different sampling steps are shown in Figures 22(d) and (e), respectively. Polymer beads of 1 µm nominal diameters were deposited on a glass slide, and the maps were acquired using a 532 nm excitation wavelength, a 100×/0.9 objective and a continuously moving XY stage. According to equation (11), the laser spot of about 0.7 µm was close to the diameter of the polymer beads. The Raman images in Figure 22(d) and (e) were generated using the MCR method that extracts spectral components corresponding to PS, PMMS and glass. These compounds are indicated, respectively, by red, yellow and black, visualizing the shape of the polymer beads in Raman images. Clearly, under-sampling at a 1.2 µm step causes image blurring and does not display the actual shape of the beads,

although it still allows the PS and PMMS parts to be discriminated. Par-sampling with the step of 0.6 µm approximately matching the size of the laser spot provides a satisfactory representation of the shape of the individual PS bead, as well as the adjacent PS and PMMA beads. Over-sampling at the 0.3 µm step results in the Raman image that more accurately depicts the shape of the polymer beads. Mapping the adjacent PS and PMMA beads at a 0.3 µm step means approximately three sampling points per the diameter of the beads. As a rule of thumb, three sampling points per object's aspects are recommended if the shape and dimensions of closely situated objects need to be well discriminated and accurately represented in the Raman image. Over-sampling by further reducing the step size leads to a minor improvement of the contrast in the Raman images but a longer acquisition time. Obviously, this recommendation applies to both the lateral and axial measurements. Note that the Raman images in Figure 22(d) and (e) slightly overestimate the sizes of the beads because the images are formed as a convolution of the original object with a laser spot of a similar size. The larger the object, the lesser the effect of the size of the laser spot on the object size estimated from the Raman spectral image.

## What is the difference between imaging and mapping Raman microscopes?

The Raman microscopes equipped with fast scanning mechanisms and usually EM-CCD detectors are often called imaging Raman microscopes. Manufacturers of Raman microscopes use this term for marketing purposes to emphasize speed and other advantages over conventional stop-and-go mode systems, which are accordingly called mapping Raman microscopes.

The imaging microscopes allow the composition and morphology of a sample to be measured and visualized in a detailed Raman spectral image in real time. They principally bring new analytical capabilities to the spectrochemical characterization of large samples on a microscopic scale. These instruments offer extraordinary productivity combined with information-reach spectral and spatial content. Due to the high scanning speed and, as a consequence, the rapid dissipation of heat, imaging Raman microscopes also ensure less laser-induced damage to sensitive samples, especially biological ones.

## What is terrain mapping?

It is important to position the sample surface in focus if the Raman spectra of the sample at the surface need to be obtained. When the sample tilt or its surface roughness exceeds the confocal depth required for the measurements, then at least part of the sample may go completely out of focus, and no meaningful spectral data will be collected from this part, as illustrated in Figure 23 (a). It may lead to the fact that the obtained spectral data will be insufficient or not representative of the sample.

Typically, flat samples are the most ideal for microscopic Raman mapping because the sample is always in focus upon sample scanning. However, the physical nature of some samples might prevent preparing a microscopically flat sample. For example, the samples, such as thin films or coatings on substrates, could be damaged or completely removed when trying to produce a flat surface. In other samples, such as natural stones and minerals, medicinal tablets and capsules, semiconductor devices, or those composed of powders or microparticles of different sizes, the preparation can result in irrevocable modifications and, consequently, the appearance of spectral artifacts.

It is also possible that irrevocable modifications of a sample are not acceptable because of the need to keep the sample intact and unaltered. Even if there are no restrictions in terms of what can be done to a sample, the methods required for producing microscopically flat samples are too complicated and time-consuming to be practical. It is, therefore, necessary to have a way of imaging rough, sloped, or uneven samples. Terrain mapping provides a way to manage these types of samples.

Terrain mapping is a technique where the vertical position of the microscope stage is adjusted to keep the sample surface in focus while acquiring Raman maps across the sample, as shown in Figure 23(b). A tightly focused laser spot provides higher laser power density, giving more Raman intensity from the analyzed volume. Maintaining a tight laser focus while moving across a sample ensures good spatial resolution and Raman intensity.

In DXR3xi Raman imaging microscope, the topography of the surface is first recorded. It is performed using the so-called optical autofocus by increasing contrast within the field of view of an objective (frame). The position of the sample in focus can be adjusted until the maximal contrast in the optical image is achieved. Suppose the area of the surface that needs to be measured exceeds the size of the single frame. In that case, the sample is scanned in the Z direction, and multiple frames at different focal points are stitched together to montage a multi-focus optical image of the sample, as outlined in Figure 23(c).
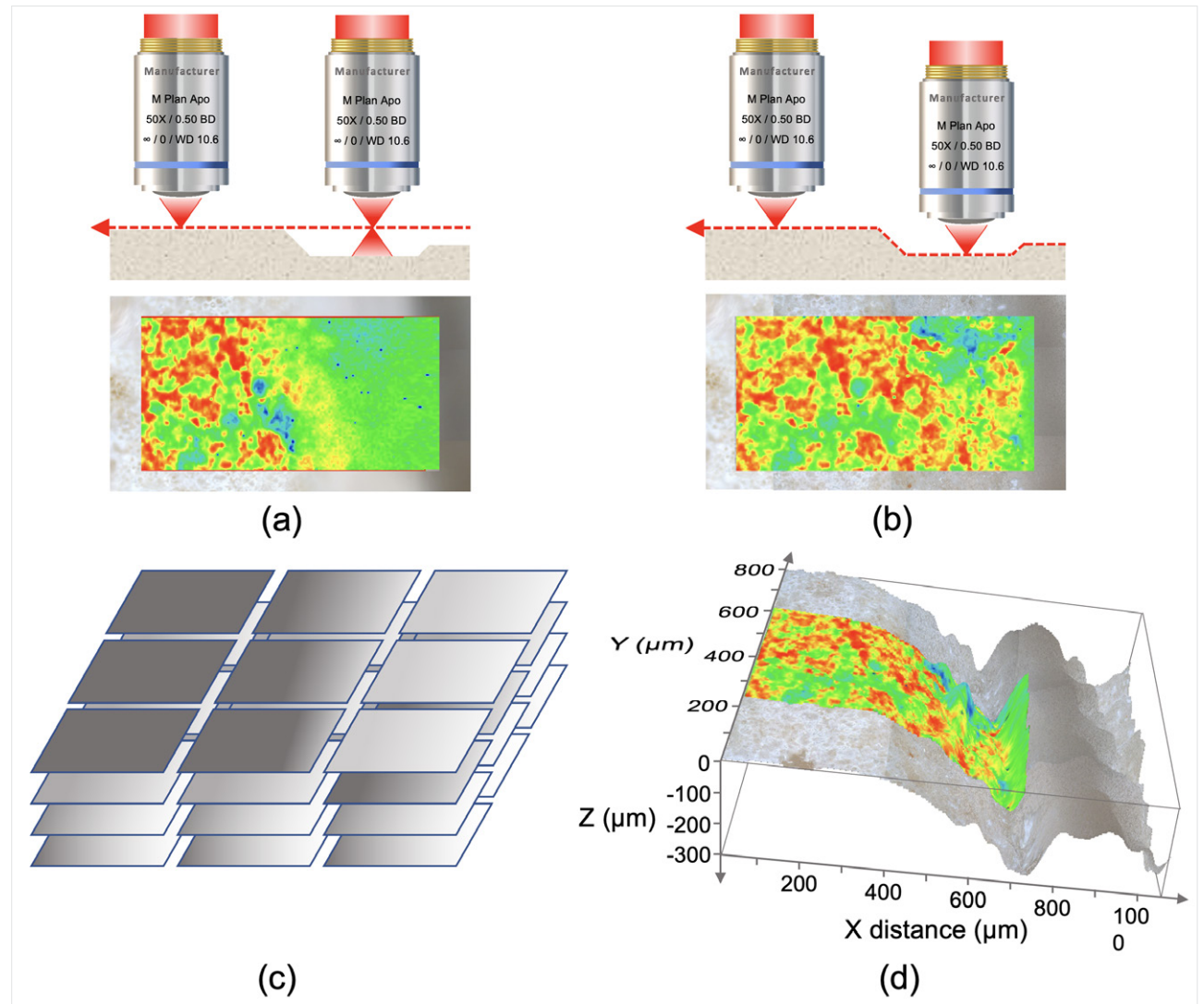


Figure 23. Mapping a part of a medicinal tablet with an uneven surface: (a) scanning the tablet at a constant Z-position of the stage; (b) scanning in Z positions adjusted to the surface profile of the tablet; (c) Mosaic tool automatically acquires the objective's field-of-view in 3D for retrieving topography of the surface; (d) the recorded topography of the tablet surface with the superimposed Raman image.

The individual frames with maximal contrast are then extracted to synthesize the topographical image in which the sample surface is maintained in focus, and the Z positions of the well-focused frames are recorded. In the second step, the Raman map is acquired at the predefined X and Y positions of the mapping grid, while the Z position at every point is retrieved from the recorded topography of the surface and dynamically adjusted during the sample scanning.

Figure 23 shows an example of the confocal analysis of an active pharmaceutical ingredient's (API) distribution in an uncoated medicinal tablet with an identification mark embossed on its surface.

The maps were acquired using a 50×/0.50 metallurgical objective and a 785 nm laser. When mapping the tablet at a constant Z position, the API distribution is adequately tracked in that part of the tablet that is well in focus. In the area of embossing, the depth of which significantly exceeds the depth of focus of the objective, the surface goes out of focus. Accordingly, the quality of the measured spectra deteriorates so that the API cannot be recognized in the out-of-focus area and distinguished from excipients (a).

Raman mapping, performed by changing the Z position of the sample stage to adjust focus to the tablet surface profile, provides confocal measurements on the uneven surface and, accordingly, adequate API tracking throughout the analyzed area, as illustrated in (b) and (d). The Raman image generated from the map obtained when the stage Z position matched the surface topography demonstrates that the API highlighted in red is distributed over the entire mapped area. The Raman images were generated as a correlation with the API's reference spectrum and superimposed on the corresponding optical images.

Learn more at **thermofisher.com/raman**

thermo scientific